phospholipase C (PI-PLC; Sigma, St. Louis, MO). The culture supernatant was harvested and concentrated at a 1/30 volume by centrifugation on a Centricon-10 filter (Millipore, Bedford, MA). Human cell lines such as HEK293 embryonal kidney cells, U-373MG astrocytoma, and NTera2 teratocarcinoma were obtained from the RIKEN Cell Bank (Tsukuba, Japan) and the American Type Culture Collection (Rockville, MD). In limited experiments, human astrocytes and U-373MG cells were incubated for 4 to 8 days in the serum-free Dulbecco's Modified Eagle's medium /F-12 medium supplemented with an insulin-transferrin-selenium supplement (Invitrogen) with or without inclusion of recombinant human IL-1β or TNFα (PeproTech EC, London, UK).

For expression of transgenes, the human *Nogo-A* gene (GenBank accession no. NM_020532) encoding the Nogo-A-specific segment (NAS; amino acids 186–1004) and the human *NgR* gene (NM_023004) encoding the full-length NgR after a cleavage of the N-terminal signal peptide (amino acids 27–473) were amplified by PCR using PfuTurbo DNA polymerase (Stratagene, La Jolla, CA) from cDNA of NTera2-derived human neurons (32) using sense and antisense primer sets (5′gatgagaccctttttgctcttcct3′ and 5′tcatgaagttttactcagctctgctga3′ for Nogo-A and 5′acgatggagagggcgtccgctggag3′ and 5′gcagggcccaagcactgtccacagcac3′ for NgR). The *Nogo-A* or *NgR* gene was cloned in an expression vector pcDNA4/HisMax-TOPO containing a N-terminal Xpress tag for detection of the recombinant protein or in pEF6/V5-His-TOPO containing a C-terminal V5 tag (Invitrogen), respectively. The vectors were transfected into HEK293 cells by using Lipofectamine 2000 reagent (Invitrogen). At 48 hours after transfection, the cells were processed for Western blot analysis.

For RT-PCR analysis, cDNA was amplified for 30 cycles by PCR using sense and antisense primer sets specific for the human NgR gene (5′cagtacctgaggctcaacgacaac3′ and 5′acctgagcctctgagtcaccagt3′; product size 588 bp) or the human glyceraldehyde-3-phosphate dehydrogenase (*G3PDH*) gene (NM_002046; 5′ccatgttcgtcatgggtgtgaacca3′ and 5′gccagtagaggcagggatgatgttc3′; the product size 251 bp) (32).

Western Blot Analysis

To prepare total protein extract, the cells and tissues were homogenized in RIPA lysis buffer composed of 50 mmol/L Tris-HCl, pH 7.5, 150 mmol/L NaCl, 1% Nonidet P40, 0.5% sodium deoxycholate, 0.1% SDS, and a cocktail of protease inhibitors (Roche Diagnostics, Mannheim, Germany), followed by centrifugation at 12,000 rpm for 20 minutes at RT. The supernatant was collected for separation on a 6%, 8%, or 12% SDS-PAGE gel. The protein concentration was determined by a Bradford assay kit (BioRad, Hercules, CA). After gel electrophoresis, the protein was transferred onto nitrocellulose membranes and immunolabeled at RT overnight with rabbit anti-Nogo-A or anti-NgR antibody. The membranes were incubated at RT for 30 minutes with horseradish peroxidase-conjugated anti-rabbit IgG (Santa Cruz Biotechnology, Santa Cruz, CA). The specific reaction was visualized with a Western blot detection system using a chemiluminescent substrate (Pierce, Rockford, IL). After the antibodies were stripped by incubating the membranes at 50°C for 30 minutes in stripping buffer composed of 62.5 mmol/L Tris-HCl, pH 6.7, 2% SDS, and 100 mmol/L 2-mercaptoethanol, the membranes were processed for relabeling with goat anti-HSP60 antibody followed by incubation with horseradish peroxidase-conjugated anti-goat IgG (Santa Cruz Biotechnology), or with mouse monoclonal anti-Xpress or anti-V5 antibody (Invitrogen) followed by incubation with horseradish peroxidase-conjugated anti-mouse IgG (Santa Cruz Biotechnology).

RESULTS

Characterization of Anti-Nogo-A and Anti-NgR Antibodies

To characterize the specificity of polyclonal anti-Nogo-A antibody (sc-25600) and anti-NgR antibody (AB5615) (Table 2), we investigated Nogo-A and NgR expression in brain homogenates by Western blot analysis. The antibody sc-25600 was raised against a peptide consisting of amino acids 700–1,000 of the human Nogo-A that represents a Nogo-A-specific internal segment not shared with Nogo-B or Nogo-C. This antibody reacted with a single band of 190-kDa protein in human and mouse brain and spinal cord homogenates (Fig. 1A). This size corresponds to that of the full-length Nogo-A of the rat oligodendrocyte lysate (11). The antibody sc-25600 recognized a 140-kDa recombinant NAS protein with an Xpress tag in the vector-transfected HEK293 cells but did not react with any proteins in nontransfected HEK293 cells (Fig. 1C). The antibody AB5615 was raised against a recombinant mouse NgR. This antibody reacted with a 64-kDa protein in human and mouse brain and spinal cord homogenates (Fig. 1B). This size corresponds to that of the full-length NgR identified in the NgR gene-transfected CHO-K1 cells and SH-SY5Y cells (33, 34). The antibody AB5615 recognized not only a 64-kDa endogenous NgR protein constitutively expressed in nontransfected HEK293 cells but also reacted with several bands immunoreactive for a V5 tag in the vector-transfected HEK293 cells (Fig. 1D). The latter might represent posttranscriptionally modified NgR isoforms. In agreement with detection of NgR in HEK293 cells on immunoblot, RT-PCR analysis using NgR-specific primer sets, which do not amplify NgR homologues NgRH1 and NgRH2 (33), identified the constitutive expression of NgR mRNA in HEK293 cells (data not shown).

Nogo-A Expression on Oligodendrocytes in Demyelinating Lesions of MS

To investigate Nogo-A expression in MS lesions, the brain, spinal cord, and optic nerve sections of 4 progressive MS patients and 12 non-MS control cases (Table 1) were processed for immunohistochemistry using the antibody sc-25600. Adjacent sections were stained with the antibodies against cell type-specific markers. In all MS cases, a substantial population (20%–60%) of surviving oligodendrocytes and remaining myelin sheath at the edge of chronic active demyelinating lesions, where numerous $CD68^+$ macrophages/microglia accumulated (Fig. 2a inset), expressed an intense immunoreactivity for Nogo-A (Table 3; Figure 2a and 2b inset). In contrast, a smaller population (< 20%) of oligodendrocytes

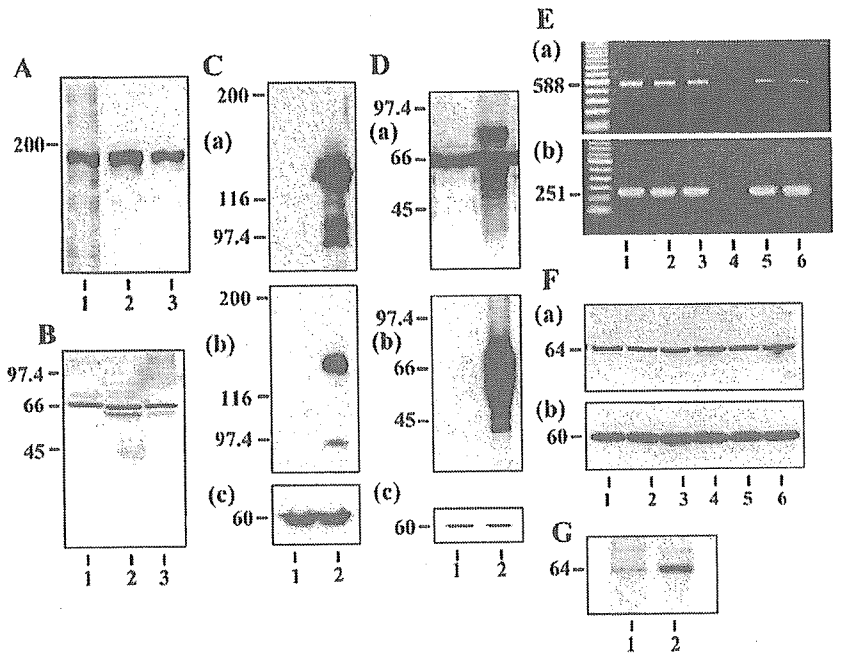

FIGURE 1. Nogo-A and NgR expression in human brain, cultured astrocytes, transfected HEK293 cells. **(A, B)** Immunoblot of brain homogenates with anti-Nogo-A **(A)** or anti-NgR **(B)** antibody. Human (lane 1) or mouse brain (lane 2), and mouse spinal cord (lane 3), 20 μg of protein each. **(C, D)** Immunoblot of HEK293 cells expressing Nogo-A-specific segment (NAS) **(C)** or NgR **(D)** with **(Ca)** anti-Nogo-A, **(Cb)** anti-Xpress, **(Da)** anti-NgR, **(Db)** anti-V5, or **(Cc and Dc)** anti-HSP60 antibody. Nontransfected (lane 1) and transfected (lane 2) HEK293 cells, 120 μg **(C)** or 4 μg **(D)** of protein each. **(E)** RT-PCR analysis of **(Ea)** NgR and **(Eb)** G3PDH mRNA in human astrocytes, astrocytoma, and teratocarcinoma cell lines. The cells were incubated for 8 days in serum-free (lanes 2, 5) or 10% FBS-containing (lanes 1, 3, 4, 6) medium. NTera2 (lane 1), cultured human astrocytes (lanes 2–4), and U-373MG (lanes 5, 6) with (lanes 1–3, 5, 6) or without (lane 4) inclusion of RT step. **(F)** Immunoblot of cultured human astrocytes with **(Fa)** anti-NgR or **(Fb)** anti-HSP60 antibody. The cells were incubated for 4 days in serum-free (lanes 1–3) or 10% FBS-containing (lanes 4–6) medium with inclusion of 100 ng/mL IL-1β (lanes 2, 5) 100 ng/mL TNF-α (lanes 3, 6) or without cytokines (lanes 1, 4), 30 μg of protein each. **(G)** Immunoblot of supernatant of cultured human astrocytes with anti-NgR antibody. The supernatant of (lane 1) untreated and (lane 2) PI-PLC-treated astrocytes.

distributed in the white matter of the brains of neurologically normal subjects displayed a fairly weak immunoreactivity for Nogo-A (Fig. 2e). An intense Nogo-A immunoreactivity was also found in surviving oligodendrocytes at the lesion border of acute and old cerebral infarction (Fig. 2d inset). The number of Nogo-A-expressing oligodendrocytes was much smaller in the center of demyelinating lesions and in the normal-appearing white matter of MS brains (Fig. 2d) and in the necrotic lesions of cerebral infarction. Double labeling immunohistochemistry verified a close association between Nogo-A-expressing oligodendrocytes and MBP, an interacting partner of Nogo-A (35) in MS lesions (Fig. 2b inset). In all MS and non-MS cases, variable Nogo-A immunoreactivity was identified in a small population (< 20%) of neurons widely distributed in the whole CNS, including motor neurons in the spinal cord with its location in the perikarya and neurites (Table 3; Fig. 2f), suggesting that not all but a substantial population of neurons in the adult human CNS express Nogo-A constitutively. In contrast, Nogo-A expression was undetectable in $GFAP^+$ reactive astrocytes (Fig. 2a, c), $CD68^+$ microglia/macrophages, ependymal cells, or $CD3^+$ T lymphocytes in chronic active demyelinating lesions of MS, ischemic lesions of cerebral infarction, and other cases (Table 3).

To investigate a possible association of Nogo-A-expressing oligodendrocytes with damaged axons in active MS lesions, adjacent sections were stained with the antibody against amyloid precursor protein (APP), a sensitive marker for acute axonal injury (21). However, APP-immunoreactive axons were hardly detectable in any cases examined (Fig. 3b), and these axons did not colocalize with Nogo-A-expressing oligodendrocytes (not shown).

NgR Expression on Reactive Astrocytes and Microglia in Demyelinating Lesions of MS

To investigate NgR expression in MS lesions, the brain, spinal cord, and optic nerve sections of 4 MS patients and 12 non-MS control cases (Table 1) were processed for immunohistochemistry using the antibody AB5615. In all MS and cerebral infarction cases, a large population (> 60%) of $GFAP^+$ reactive astrocytes and $CD68^+$ microglia/macrophages that accumulated in chronic active and inactive demyelinating lesions or in ischemic lesions expressed an intense immunoreactivity for NgR (Table 3; Fig. 4a, d, e). Furthermore, a fairly small number of $GFAP^+$ astrocytes and $CD68^+$ microglia, occasionally found in the brains of neurologically normal subjects, were also stained intensely with anti-NgR antibody (Fig. 4d inset). These observations suggest that both astrocytes and microglia express high levels of NgR, particularly when they become activated. Double-labeling immunohistochemistry verified coexpression of NgR and GFAP on reactive astrocytes in demyelinating lesions of MS (Fig. 3c, d). In all MS and non-MS cases, variable NgR immunoreactivity was identified in a large population (> 60%) of neurons and their neurites widely distributed in the whole CNS (Table 3; Fig. 4f), suggesting that not all but a wide variety of neurons in the adult human CNS constitutively express high levels of NgR. Among them, cerebral cortical neurons and spinal cord motor neurons coexpressed Nogo-A and NgR (Figs. 2f, 4f). In addition,

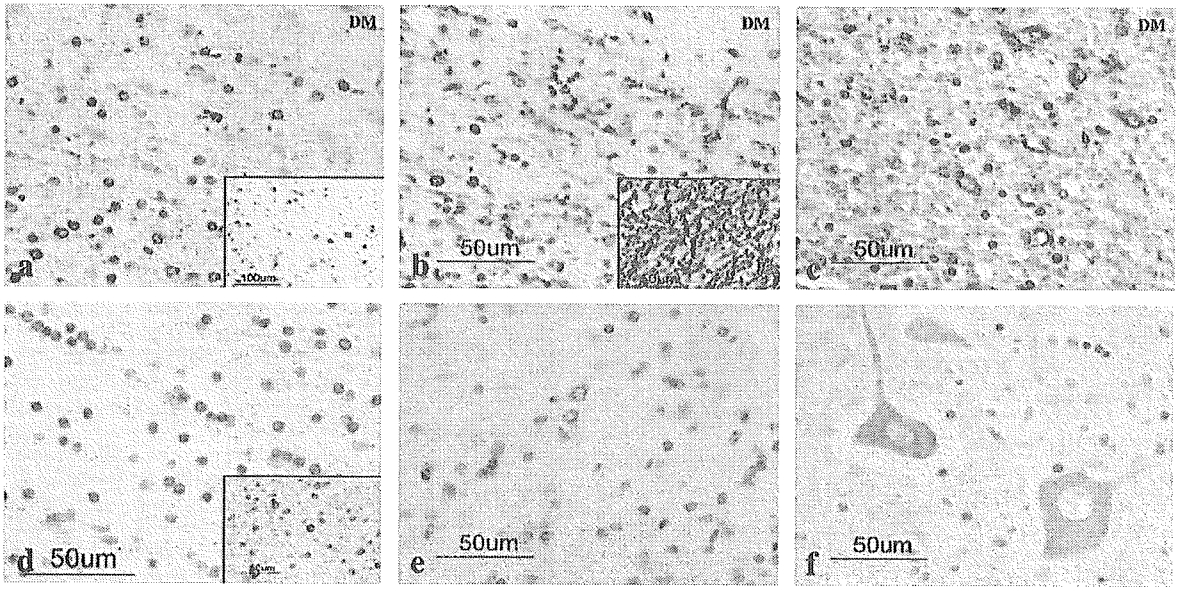

FIGURE 2. Nogo-A expression on oligodendrocytes in demyelinating lesions of MS. Immunohistochemistry. **(a)** No. 744 MS, Nogo-A, the edge of chronic active demyelinating lesions (DM) in the subcortical white matter of the frontal lobe (inset, CD68). **(b)** No. 744 MS, MBP, the adjacent section of panel a (inset, no. 791 MS, double immunolabeling for Nogo-A as red and MBP as brown). **(c)** No. 744 MS, GFAP, the adjacent section of panel a. **(d)** No. 744 MS, Nogo-A, the normal-appearing white matter of the frontal lobe (inset, no. 786 acute cerebral infarction, Nogo-A, the lesion border in the subcortical white matter of the parietal lobe). **(e)** No. A2647 neurologically normal subject, Nogo-A, the subcortical white matter of the frontal lobe. **(f)** No. 791 MS, Nogo-A, motor neurons in the spinal cord.

ependymal cells constitutively expressed intense NgR immunoreactivity, while NgR expression was not found in oligodendrocytes (Table 3; Fig. 4a, c) or $CD3^+$ T lymphocytes.

In contrast to widespread distribution of NgR in the human CNS, the NgR coreceptor $p75^{NTR}$ immunoreactivity was identified in fairly restricted regions: most prominently expressed in nerve fibers of substantia gelatinosa in the spinal cord (Fig. 3a), tractus solitarius in the brainstem, and found in the vascular wall in the cerebrum. $p75^{NTR}$ was not expressed on oligodendrocytes, astrocytes, or microglia/macrophages in any cases examined (not shown).

Constitutive Expression of NgR in Cultured Human Astrocytes

Because a previous study did not identify NgR on astrocytes in the human CNS (15), NgR expression was studied in cultured human astrocytes to verify the present observations. RT-PCR analysis using NgR-specific primer sets identified a substantial level of NgR mRNA in human astrocytes in culture, along with U-373MG and NTera2 cells (Fig. 1E). No products were amplified when total RNA was processed for PCR omitting RT step, confirming that a contamination of genomic DNA was excluded (Fig. 1E, lane 4). By Western blot analysis, NgR protein levels were unaltered in cultured human astrocytes by exposure to IL-1β or TNFα under the serum-free or serum-containing culture condition, when standardized against the levels of HSP60, a housekeeping gene product, detected on the identical blots (Fig. 1F). Double labeling immunocytochemistry verified coexpression of NgR and GFAP in cultured human astrocytes, where a substantial NgR immunoreactivity was identified in the cytoplasm (Fig. 3e, f). Furthermore, a large amount of NgR protein was detected in the supernatant of PI-PLC-treated

TABLE 3. Differential Expression of Nogo-A and Nogo Receptor in Glial Cells and Neurons in MS and Control Brains

Brain	Astrocytes			Microglia/Macrophages			Oligodendrocytes			Neurons		
	MS	OND	NNC	MS	OND	NNC	MS	OND	NNC	MS	OND	NNC
Nogo-A	n(−)	n(−)	n(−)	n(−)	n(−)	n(−)	m(++)	m(++)	s(+)	s(+/++)	s(+)	s(+)
NgR	l(++)	l(++)	l*(++)	l(++)	l(++)	l*(++)	n(−)	n(−)	n(−)	l(+/++)	l(+/++)	l(+/++)

The present study includes 4 MS cases, 6 non-MS neurologic and psychiatric disease cases (OND), and 6 neurologically normal cases (NNC), as shown in Table 1. The population size of immunoreactive cells per total is expressed as [l] large (>60%); [m] moderate (60–20%); [s] small (<20%), [n] almost none, and [l*] large population but small number. The intensity of immunoreactivity is graded as (−) negative, (+) weak, (++) intense, and (+/++) variable.

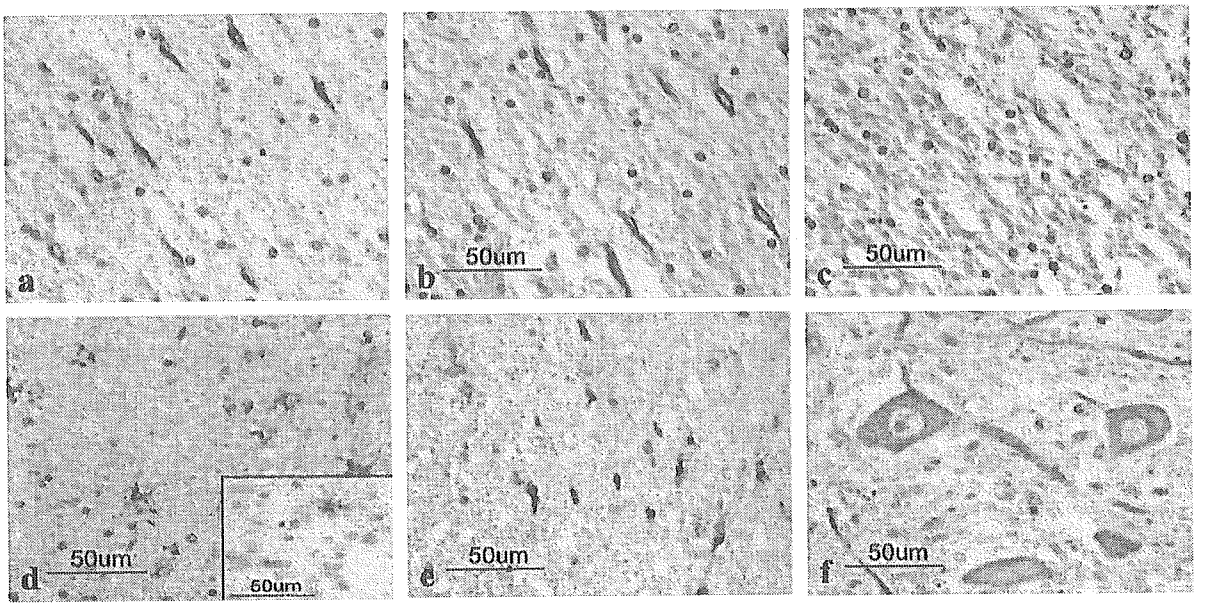

FIGURE 3. NgR expression on reactive astrocytes and microglia in demyelinating lesions of MS. Immunohistochemistry. **(a)** No. 744 MS, NgR, the edge of chronic active demyelinating lesions in the subcortical white matter of the frontal lobe. **(b)** No. 744 MS, GFAP, the adjacent section of panel a. **(c)** No. 744 MS, MBP, the adjacent section of panel a. **(d)** No. 791 MS, NgR, chronic active demyelinating lesions in the pons (inset, no. A2647 neurologically normal subject, NgR, the subcortical white matter of the frontal lobe). **(e)** No. 744 MS, NgR, chronic active demyelinating lesions in the pons. **(f)** No. 744 MS, NgR, motor neurons in the spinal cord.

human astrocyte cultures (Fig. 1G, lane 2), although a small amount of NgR was found in that of untreated cultures (Fig. 1G, lane 1).

DISCUSSION

The present study showed that Nogo-A expression was markedly upregulated in surviving oligodendrocytes, while NgR expression was greatly enhanced in reactive astrocytes and microglia/macrophages in chronic active demyelinating lesions of MS and ischemic lesions of acute and old cerebral infarction, when compared with their expression in the brains of neurologically normal controls. Both Nogo-A and NgR were also identified in a subpopulation of neurons in the brain and spinal cord, consistent with previous observations (4–9, 14, 15). In contrast, Nogo-A was undetectable in reactive astrocytes and microglia/macrophages, and NgR was not virtually expressed on oligodendrocytes. Previous studies suggested that Nogo-A released from injured oligodendrocytes and damaged myelin sheath in the CNS lesions acts on neighboring NgR-expressing neurons and their axons (36). Our observations raise an alternative possibility that Nogo-A expressed on surviving oligodendrocytes interacts directly with NgR presented by reactive astrocytes and microglia/macrophages at the site of active demyelinating lesions of MS. A possible role of NgR on reactive astrocytes and microglia includes an inhibition of their proliferation, down-regulation of cytokine production, and sequestration of Nogo-A released from damaged oligodendrocytes by acting as a non-functioning decoy receptor.

The regulatory mechanism for Nogo-A and NgR expression remains largely unknown. Several studies suggested that Nogo-A and NgR levels are not substantially altered in the adult rodent CNS following injury (4, 6, 14). The CNS injury is often accompanied by a local infiltration of lymphocytes and macrophages and an activation of microglia and astrocytes, all of which provide a source of reactive oxygen species, pro-inflammatory cytokines, and neurotrophic factors. Previously, we found that Nogo-A and NgR mRNA levels are unaffected in human neurons in culture by exposure to basic FGF, BDNF, GDNF, IL-1β, or TNF-α, despite their expression of specific receptors (32). The present study revealed that human astrocytes in culture constitutively express NgR, whose levels remain unchanged by treatment with IL-1β or TNFα. Recent studies showed that the expression of Nogo-A but not of NgR is regulated by stress-inducing stimuli. Global ischemia enhances Nogo-A expression on the myelin sheath in the adult rat brain (37), supporting the present observations. In contrast, neonatal hypoxia reduces Nogo-A protein levels on oligodendrocytes in a mouse model (38). Nogo-A expression is markedly reduced at CNS paranodes in the rats affected with experimental autoimmune encephalomyelitis (39). Nogo-A expression is upregulated around the lesion site, whereas NgR is maintained at constant levels in the adult mouse and rat spinal cord following injury (5, 8). Nogo-A mRNA levels are elevated in the adult rat hippocampal neurons after kainate-induced seizure (40). Furthermore, Nogo-A is induced in hippocampal neurons of the patients with temporal lobe epilepsy (41). Nogo-A is upregulated in denervated and innervated mouse skeletal muscle and in postmortem and biopsied muscles of amyotrophic lateral sclerosis patients (42, 43).

The human Nogo-A/B promoter lacks a typical TATA-box and consensus sequences for known oligodendrocyte-specific

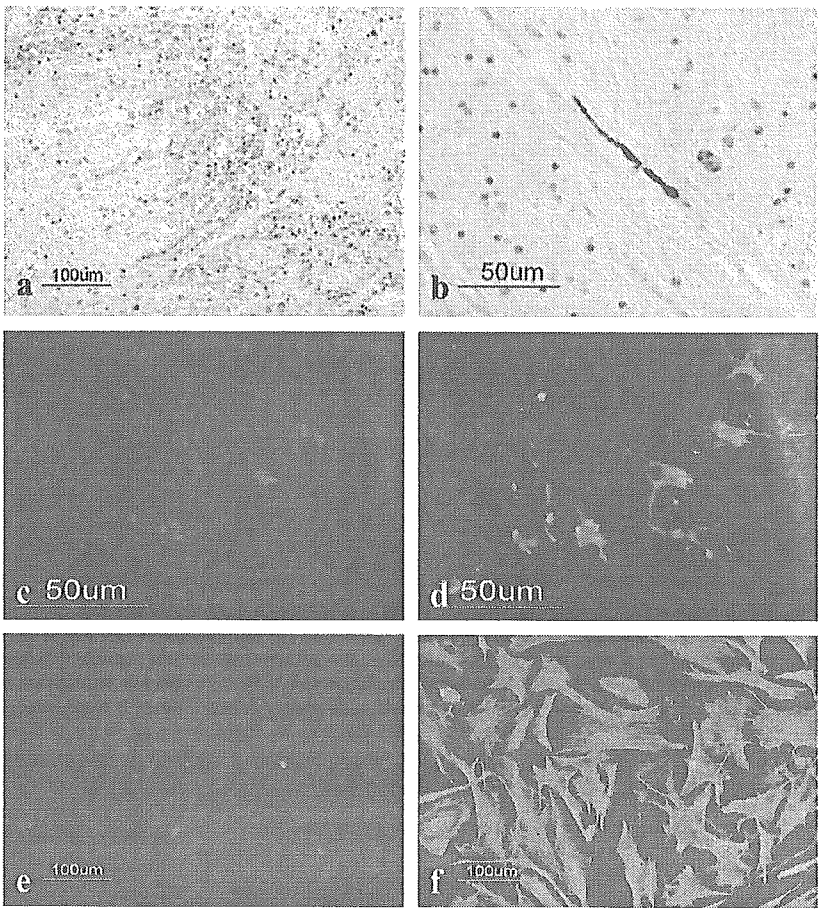

FIGURE 4. Coexpression of NgR and GFAP on reactive astrocytes in MS lesions and cultured human astrocytes. Immunohistochemistry and immunocytochemistry. **(a)** No. 791 MS, $p75^{NTR}$, the substantia gelatinosa in the spinal cord. **(b)** No. 609 MS, APP, chronic active demyelinating lesions in the medulla oblongata. **(c, d)** No. 744 MS, double immunolabeling for NgR (red) and GFAP (green), chronic active demyelinating lesions in the subcortical white matter of the frontal lobe. **(e, f)** Cultured human astrocytes, double immunolabeling for NgR (red) and GFAP (green).

transcription factors, but it has a CpG island where a number of CpG sequences are frequently methylated (10). Such GC-rich promoters are typically identified in housekeeping genes whose expression is ubiquitous. However, multiple GC-boxes within the promoter region might lead to a synergistic activation by the Sp1 family of oligodendrocyte-specific or neuron-specific transcription factors (10). Interestingly, several nonneural cell lines such as 3T3 fibroblasts and C2 myoblasts express Nogo-A, where no direct correlation is observed between Nogo-A mRNA and protein levels (10). On the other hand, the human NgR promoter has not at present been characterized. An in situ hybridization study showed that NgR is undetectable in the spinal cord, and not expressed in ependymal cells, but identified in a subpopulation of neurons in the neocortex, hippocampus, amygdala, and the dorsal root ganglia in the adult human CNS (15). The discrepancy between this study and our own is attributable to the differences in brain tissues examined and the methods applied for identification of NgR. Recent studies showed that a subset of CNS neurons, including motor neurons in the adult rat and mouse spinal cord, coexpress NgR and Nogo-A (4, 8, 14), supporting the present observations. In addition, both Nogo-A and NgR are identified in the human spinal cord during development when Nogo-A does not play a negative role in regeneration (44). Most importantly, NgR expression is not confined to neurons. U87MG human glioblastoma cells express a great amount of endogenous NgR, through which Nogo-66 modulates their growth and migration (45). Although the LRR, LRRCT, and LRRNT subdomains of NgR are all involved in ligand binding (46), the DNAQLR motif located in the third LRR domain is identified as the principal epitope recognized by a monoclonal anti-NgR antibody capable of blocking binding of all NgR ligands (47). We found that a substantial NgR immunoreactivity was located in the cytoplasm of cultured human astrocytes, in addition to the detection of NgR protein in the supernatant of PI-PLC-treated and untreated cultures. The intracellular localization of NgR appears unusual, but it might reflect the changes in cell–cell interactions under culture conditions (44). Supporting our observations, an immunoelectron microscopic analysis showed that NgR is located at both presynaptic and postsynaptic regions where NgR-immunoreactive products distribute diffusely among cytoplasmic elements including synaptic vesicles, mitochondria, and microtubules (5). Furthermore, in human neuroblastoma cells, NgR is constitutively cleaved in a post-ER compartment by zinc metalloproteinases, and a

resulting soluble N-terminal fragment is released into the culture medium (34).

The NgR coreceptor $p75^{NTR}$ transducing the signals from Nogo-66, MAG, and OMgp via NgR (16, 17) acts as a displacement factor that releases Rho from the Rho GDP dissociation inhibitor (Rho-GDI) (48). Neurons lacking $p75^{NTR}$ neither show RhoA activation nor exhibit neurite growth inhibition in the presence of myelin components (16). In general, $p75^{NTR}$ is expressed at high levels in neurons and glial cells during development, while its expression level declines to background levels in the adult CNS (49). However, $p75^{NTR}$ is reexpressed in the adult CNS following injury, ischemia, and inflammation (50). Previous studies by immunohistochemistry using a polyclonal anti-$p75^{NTR}$ antibody (G323A, Promega) showed that $p75^{NTR}$ is expressed on oligodendrocytes and microglia/macrophages in active MS lesions (51, 52). In contrast, the present study using the monoclonal antibody ME20.4 showed that $p75^{NTR}$ expression was limited in some regions such as substantia gelatinosa in the spinal cord, as described previously (53). A recent study showed that the antibody G323A exhibits a broad reactivity with numerous cross-reactive bands in PNS and CNS homogenates (54). Our observations support the view that NgR and $p75^{NTR}$ distribution does not always overlap in the CNS. NgR is identified in many cell types in the adult CNS that exhibit little or no $p75^{NTR}$ expression, whereas $p75^{NTR}$-expressing central cholinergic neurons in the medial septal nucleus do not express NgR (14). The depletion of $p75^{NTR}$ does not promote axonal regeneration after spinal cord injury (55), suggesting that an unidentified coreceptor for NgR might act as an alternative transducer of neurite growth-inhibitory signals (49). Another possibility exists that no alternative coreceptor is expressed in NgR-expressing cells where NgR acts as a nonsignaling receptor to take up an excessive amount of extracellularly released Nogo. Importantly, the NgR/$p75^{NTR}$ receptor complex is not required for mediating the neurite growth-inhibitory activity of the NAS domain of Nogo-A (56).

In conclusion, Nogo-A expression was upregulated in surviving oligodendrocytes, while NgR expression was enhanced in reactive astrocytes and microglia/macrophages in chronic active demyelinating lesions of MS, although the functional significance of these observations remains to be further investigated.

ACKNOWLEDGMENTS

The authors thank Dr. Mitsuru Kawai, Department of Neurology, National Center Hospital for Mental, Nervous and Muscular Disorders, NCNP, Tokyo, Japan for providing information about MS patients; Dr. Toshikazu Murakami, Department of Pathology, Kohnodai Hospital, NCNP, Chiba, Japan for providing the brains of neurologically normal controls; and Dr. Seiichi Haga, Department of Schizophrenia Research, Tokyo Institute of Psychiatry, Tokyo, Japan for providing anti-APP antibody.

REFERENCES

1. Schwab ME, Bartholdi D. Degeneration and regeneration of axons in the lesioned spinal cord. Physiol Rev 1996;76:319–70
2. Chen MS, Huber AB, van der Haar ME, et al. Nogo-A is a myelin-associated neurite outgrowth inhibitor and an antigen for monoclonal antibody IN-1. Nature 2000;403:434–39
3. GrandPré T, Nakamura F, Vartanian T, et al. Identification of the Nogo inhibitor of axon regeneration as a Reticulon protein. Nature 2000;403:439–44
4. Huber AB, Weinmann O, BrösamLe C, et al. Patterns of Nogo mRNA and protein expression in the developing and adult rat and after CNS lesions. J Neurosci 2002;22:3553–67
5. Wang X, Chun S-J, Treloar H, et al. Localization of Nogo-A and Nogo-66 receptor proteins at sites of axon-myelin and synaptic contact. J Neurosci 2002;22:5505–15
6. Josephson A, Widenfalk J, Widmer HW, et al. NOGO mRNA expression in adult and fetal human and rat nervous tissue and in weight drop injury. Exp Neurol 2001;169:319–28
7. Liu H, Ng CEL, Tang BL. Nogo-A expression in mouse central nervous system neurons. Neurosci Lett 2002;328:257–60
8. Hunt D, Coffin RS, Prinjha RK, et al. Nogo-A expression in the intact and injured nervous system. Mol Cell Neurosci 2003;24:1083–102
9. Liu Y-Y, Jin W-L, Liu H-L, et al. Electron microscopic localization of Nogo-A at the postsynaptic active zone of the rat. Neurosci Lett 2003;346:153–56
10. Oertle T, Huber C, van der Putten H, et al. Genomic structure and functional characterisation of the promoters of human and mouse *nogo/rtn4*. J Mol Biol 2003;325:299–323
11. Oertle T, van der Haar ME, Bandtlow CE, et al. Nogo-A inhibits neurite outgrowth and cell spreading with three discrete regions. J Neurosci 2003; 23:5393–406
12. Fournier AE, GrandPre T, Strittmatter SM. Identification of a receptor mediating Nogo-66 inhibition of axonal regeneration. Nature 2001;409:341–46
13. He XL, Bazan F, McDermott G, et al. Structure of the Nogo receptor ectodomain: A recognition module implicated in myelin inhibition. Neuron 2003;38:177–85
14. Hunt D, Mason MRJ, Campbell G, et al. Nogo receptor mRNA expression in intact and regenerating CNS neurons. Mol Cell Neurosci 2002;20: 537–52
15. Josephson A, Trifunovski A, Widmer HR, et al. Nogo-receptor gene activity: Cellular localization and developmental regulation of mRNA in mice and humans. J Comp Neurol 2002;453:292–304
16. Wang KC, Kim JA, Sivasankaran R, et al. p75 interacts with the Nogo receptor as a co-receptor for Nogo, MAG and OMgp. Nature 2002;420:74–78
17. Niederöst B, Oertle T, Fritsche J, et al. Nogo-A and myelin-associated glycoprotein mediate neurite growth inhibition by antagonistic regulation of RhoA and Rac1. J Neurosci 2002;22:10368–76
18. Bareyre FM, Haudenschild B, Schwab ME. Long-lasting sprouting and gene expression changes induced by the monoclonal antibody IN-1 in the adult spinal cord. J Neurosci 2002;22:7097–110
19. Fournier AE, Gould GC, Liu BP, et al. Truncated soluble Nogo receptor binds to Nogo-66 and blocks inhibition of axonal growth by myelin. J Neurosci 2002;22:8876–83
20. GrandPré T, Li S, Strittmatter SM. Nogo-66 receptor antagonist peptide promotes axonal regeneration. Nature 2002;417:547–51
21. Ferguson B, Matyszak MK, Esiri MM, et al. Axonal damage in acute multiple sclerosis lesions. Brain 1997;120:393–99
22. Trapp BD, Peterson J, Ransohoff RM, et al. Axonal transection in the lesions of multiple sclerosis. N Engl J Med 1998;338:278–85
23. Reindl M, Khantane S, Ehling R, et al. Serum and cerebrospinal fluid antibodies to Nogo-A in patients with multiple sclerosis and acute neurologic disorders. J Neuroimmunol 2003;145:139–47
24. Buffo A, Zagrebelsky M, Huber AB, et al. Application of neutralizing antibodies against NI-35/250 myelin-associated neurite growth inhibitory proteins to the adult rat cerebellum induces sprouting of uninjured Purkinje cell axons. J Neurosci 2000;20:2275–86
25. Emerick AJ, Neafsey EJ, Schwab ME, et al. Functional reorganization of the motor cortex in adult rats after cortical lesion and treatment with monoclonal antibody IN-1. J Neurosci 2003;23:4826–30
26. Kim J-E, Li S, Grandpré T, et al. Axon regeneration in young adult mice lacking Nogo-A/B. Neuron 2003;38:187–99
27. Simonen M, Pedersen V, Weinmann O, et al. Systemic deletion of the myelin-associated outgrowth inhibitor Nogo-A improves regenerative and plastic responses after spinal cord injury. Neuron 2003;38:201–11

28. Zheng B, Ho C, Li S, et al. Lack of enhanced spinal regeneration in Nogo-deficient mice. Neuron 2003;38:213–24
29. Karnezis T, Mandemakers W, McQualter JL, et al. The neurite outgrowth inhibitor Nogo A is involved in autoimmune-mediated demyelination. Nat Neurosci 2004;7:736–44
30. Lee J-K, Kim J-E, Sivula M, et al. Nogo receptor antagonism promotes stroke recovery by enhancing axonal plasticity. J Neurosci 2004;24: 6209–17
31. Satoh J-I, Yamamura T, Arima K. The 14-3-3 protein ε isoform expressed in reactive astrocytes in demyelinating lesions of multiple sclerosis binds to vimentin and glial fibrillary acidic protein in cultured human astrocytes. Am J Pathol 2004;165:577–92
32. Satoh J-I, Kuroda Y. Cytokines and neurotrophic factors fail to affect Nogo-A mRNA expression in differentiated human neurones: implications for inflammation-related axonal regeneration in the central nervous system. Neuropathol Appl Neurobiol 2002;28: 95–106
33. Pignot V, Hein AE, Barske C, et al. Characterization of two novel proteins, NgRH1 and NgRH2, structurally and biochemically homologous to the Nogo-66 receptor. J Neurochem 2003;85:717–28
34. Walmsley AR, McCombie G, Neumann U, et al. Zinc metalloproteinase-mediated cleavage of the human Nogo-66 receptor. J Cell Sci 2004; 117:4591–602
35. Taketomi M, Kinoshita N, Kimura K, et al. Nogo-A expression in mature oligodendrocytes of rat spinal cord in association with specific molecules. Neurosci Lett 2002;332:37–40
36. Ng CEL, Tang BL. Nogos and the Nogo-66 receptor: Factors inhibiting CNS neuron regeneration. J Neurosci Res 2002;67:559–65
37. Zhou C, Li Y, Nanda A, et al. HBO suppresses Nogo-A, Ng-R, or RhoA expression in the cerebral cortex after global ischemia. Biochem Biophys Res Commun 2003;309:368–76
38. Weiss J, Takizawa B, McGee A, et al. Neonatal hypoxia suppresses oligodendrocyte Nogo-A and increases axonal sprouting in a rodent model for human prematurity. Exp Neurol 2004;189:141–49
39. Nie D-Y, Zhou Z-H, Ang B-T, et al. Nogo-A at CNS paranodes is a ligand of Caspr: Possible regulation of K^+ channel localization. EMBO J 2003;22:5666–78
40. Meier S, Bräuer AU, Heimrich B, et al. Molecular analysis of Nogo expression in the hippocampus during development and following lesion and seizure. FASEB J 2003;17:1153–55
41. Bandtlow CE, Dlaska M, Pirker S, et al. Increased expression of Nogo-A in hippocampal neurons of patients with temporal lobe epilepsy. Eur J Neurosci 2004;20:195–206
42. Dupuis L, de Aguilar J-LG, di Scala F, et al. Nogo provides a molecular marker for diagnosis of amyotrophic lateral sclerosis. Neurobiol Dis 2002;10:358–65
43. Magnusson C, Libelius R, Tågerud S. Nogo (Reticulon 4) expression in innervated and denervated mouse skeletal muscle. Mol Cell Neurosci 2003;22:298–307
44. O'Neill P, Whalley K, Ferretti P. Nogo and Nogo-66 receptor in human and chick: implications for development and regeneration. Dev Dyn 2004;231:109–21
45. Liao H, Duka T, Teng FYH, et al. Nogo-66 and myelin-associated glycoprotein (MAG) inhibit the adhesion and migration of Nogo-66 receptor expressing human glioma cells. J Neurochem 2004;90:1156–62
46. Barton WA, Liu BP, Tzvetkova D, et al. Structure and axon outgrowth inhibitor binding of the nogo-66 receptor and related proteins. EMBO J 2003;22:3291–302
47. Li W, Walus L, Rabacchi SA, et al. A neutralizing anti-Nogo66 receptor monoclonal antibody reverses inhibition of neurite outgrowth by central nervous system myelin. J Biol Chem 2004;279:43780–88
48. Yamashita T, Tohyama M. The p75 receptor acts as a displacement factor that releases Rho from Rho-GDI. Nat Neurosci 2003;6:461–67
49. He Z, Koprivica V. The Nogo signaling pathway for regeneration block. Annu Rev Neurosci 2004;27:341–68
50. Dechant G, Barde Y-A. The neurotrophin receptor $p75^{NTR}$: Novel functions and implications for diseases of the nervous system. Nat Neurosci 2002;5:1131–36
51. Dowling P, Ming X, Raval S, et al. Upregulated $p75^{NTR}$ neurotrophin receptor on glial cells in MS plaques. Neurology 1999;53:1676–82
52. Chang A, Nishiyama A, Peterson J, et al. NG2-positive oligodendrocyte progenitor cells in adult human brain and multiple sclerosis lesions. J Neurosci 2000;20:6404–12
53. Mufson EJ, Brashers-Krug T, Kordower JH. p75 nerve growth factor receptor immunoreactivity in the human brainstem and spinal cord. Brain Res 1992;589:115–23
54. Valdo P, Stegagno C, Mazzucco S, et al. Enhanced expression of NGF receptors in multiple sclerosis lesions. J Neuropathol Exp Neurol 2002; 61:91–98
55. Song X-Y, Zhong J-h, Wang X, et al. Suppression of p75NTR does not promote regeneration of injured spinal cord in mice. J Neurosci 2004; 24:542–46
56. Schweigreiter R, Walmsley AR, Niederöst B, et al. Versican V2 and the central inhibitory domain of Nogo-A inhibit neurite growth via $p75^{NTR}$/NgR-independent pathways that converge at RhoA. Mol Cell Neurosci 2004;27:163–74

J Neuropathol Exp Neurol

ORIGINAL ARTICLE

The 14-3-3 Protein Forms a Molecular Complex with Heat Shock Protein Hsp60 and Cellular Prion Protein

Jun-ichi Satoh, MD, PhD, Hiroyuki Onoue, MD, PhD, Kunimasa Arima, MD, PhD, and Takashi Yamamura, MD, PhD

Abstract

The 14-3-3 protein family consists of acidic 30-kDa proteins composed of 7 isoforms expressed abundantly in neurons and glial cells of the central nervous system (CNS). The 14-3-3 protein identified in the cerebrospinal fluid provides a surrogate marker for premortem diagnosis of Creutzfeldt-Jakob disease, although an active involvement of 14-3-3 in the pathogenesis of prion diseases remains unknown. By protein overlay and mass spectrometric analysis of protein extract of NTera2-derived differentiated neurons, we identified heat shock protein Hsp60 as a 14-3-3-interacting protein. The 14-3-3ζ and γ isoforms interacted with Hsp60, suggesting that the interaction is not isoform-specific. Furthermore, the interaction was identified in SK-N-SH neuroblastoma, U-373MG astrocytoma, and HeLa cervical carcinoma cells. The cellular prion protein (PrPC) along with Hsp60 was coimmunoprecipitated with 14-3-3 in the human brain protein extract. By protein overlay, 14-3-3 interacted with both recombinant human Hsp60 and PrPC produced by *Escherichia coli*, indicating that the molecular interaction is phosphorylation-independent. The 14-3-3-binding domain was located in the N-terminal half (NTF) of Hsp60 spanning amino acid residues 27–287 and the NTF of PrPC spanning amino acid residues 23–137. By immunostaining, the 14-3-3 protein Hsp60 and PrPC were colocalized chiefly in the mitochondria of human neuronal progenitor cells in culture, and were coexpressed most prominently in neurons and reactive astrocytes in the human brain. These observations indicate that the 14-3-3 protein forms a molecular complex with Hsp60 and PrPC in the human CNS under physiological conditions and suggest that this complex might become disintegrated in the pathologic process of prion diseases.

Key Words: 14-3-3, Hsp60, Mass spectrometry, Prion protein, Protein overlay.

From the Department of Immunology (J-IS, HO, TY), National Institute of Neuroscience, NCNP, Tokyo, Japan; and Department of Neuropathology (KA), National Center Hospital for Mental, Nervous, and Muscular Disorders, NCNP, Tokyo, Japan.

Send correspondence and reprint requests to: Dr. Jun-ichi Satoh, Department of Immunology, National Institute of Neuroscience, NCNP, 4-1-1 Ogawahigashi, Kodaira, Tokyo 187-8502, Japan; E-mail: satoj@ncnp.go.jp

This work is supported by the Grant-in-Aid for Scientific Research (B2-15390280 and PA007-16017320), the Ministry of Education, Science, Sports and Culture; Research on Psychiatric and Neurological Diseases and Mental Health, the Ministry of Health, Labour and Welfare of Japan (H17-020); Research on Health Sciences Focusing on Drug Innovation, the Japan Health Sciences Foundation (KH21101); and the Organization for Pharmaceutical Safety and Research (OPS) Kiko, Japan.

INTRODUCTION

The 14-3-3 protein family consists of evolutionarily conserved, acidic 30-kDa proteins composed of seven isoforms named β, γ, ε, ζ, η, θ, and σ in eukaryotic cells. A homodimeric or heterodimeric complex composed of the same or distinct isoforms constitutes a large cup-like structure possessing an amphipathic groove with two ligand-binding capacity (1, 2). The dimeric complex acts as a molecular adaptor that interacts with key signaling molecules involved in cell differentiation, proliferation, transformation, and apoptosis. The 14-3-3 protein regulates the function of target proteins by restricting their subcellular location, bridging them to modulate catalytic activity and protecting them from dephosphorylation or proteolysis (3, 4). Although the 14-3-3 protein is widely distributed in neural and nonneural tissues, it is expressed most abundantly in neurons in the central nervous system (CNS), where it represents 1% of total cytosolic proteins (5).

In general, the 14-3-3 protein interacts with phosphoserine-containing motifs of the ligands such as RSXpSXP (mode I) and RXXXpSXP (mode II) in a sequence-specific manner (3, 4). More than 300 proteins, amounting to approximately 0.6% of the human proteome, have been identified as being 14-3-3-binding partners. They include Raf-1 kinase, Bcl-2 antagonist of cell death (BAD), protein kinase C (PKC), phosphatidylinositol 3-kinase (PI3K), cdc25 phosphatase, glycogen synthase kinase-3β (GSK3β), α-synuclein, and ataxin-1 (6–9). Binding of the 14-3-3 protein to Raf-1 is indispensable for its kinase activity in the Ras-MAPK signaling pathway, whereas the interaction of 14-3-3 with BAD, when phosphorylated by a serine/threonine kinase Akt, inhibits apoptosis (1, 2). The target proteins for 14-3-3 are distributed in all subcellular compartments (3, 9). In addition to the phosphorylation-dependent interaction, the 14-3-3 protein occasionally interacts with a set of target proteins in a phosphorylation-independent manner (10–13).

Recently, the 14-3-3 protein detected in the cerebrospinal fluid (CSF) of Creutzfeldt-Jacob disease (CJD) has been used as a biochemical marker that strongly supports the diagnosis of CJD (14, 15). Furthermore, an intense immunoreactivity against the 14-3-3ζ isoform was identified in amyloid plaques in the CJD brain (16). However, it remains unknown whether the 14-3-3 protein plays an active role in the development of prion diseases. The great majority of prion diseases are characterized by intracerebral accumulation of an abnormal prion protein (PrPSc) that is identical in the amino acid sequence to the cellular isoform (PrPC) encoded by the

PRNP gene. PrPSc differs biochemically from PrPC by its β-sheet-enriched structure, detergent insolubility, limited proteolysis by proteinase K, and a slower turnover rate (17). Previous studies suggest that the conversion of PrPC into PrPSc is mediated by a homotypic interaction between endogenous PrPC and incoming or de novo-generated PrPSc through an undefined posttranslational process (17).

Heat shock protein (Hsp) acts as a molecular chaperone that plays an essential role in protein folding, transport, degradation, and signal transduction and is pivotal for recovery from stress-induced protein damage (18). Hsp60, alternatively named as chaperonin 60 (Cpn60), recognizes exposed hydrophobic surfaces of various proteins with globular nonnative conformations, binds them in the central cavity, and stabilizes them against irreversible denaturation and aggregation (19, 20). Dysregulation of Hsp function is supposed to be involved in the pathogenesis of neurodegenerative diseases characterized by an accumulation of intracellular and extracellular protein aggregates (21). A missense mutation in Hsp60 that causes a loss of chaperone function is responsible for an autosomal-dominant form of hereditary spastic paraplegia (22). Several lines of evidence suggest that Hsp60 promotes the conversion of PrPC to PrPSc in vitro, although it remains unknown whether PrPC and Hsp60 could interact in vivo in the same subcellular compartment (23, 24).

The present study, by using protein overlay and mass spectrometry analysis, identified Hsp60 as a 14-3-3-interacting protein in human neurons. Furthermore, PrPC along with Hsp60 was coimmunoprecipitated with 14-3-3 in the human brain protein extract, and they were colocalized chiefly in the mitochondria of human neural cells in culture and coexpressed most prominently in neurons and astrocytes in the human brain. These observations indicate that the 14-3-3 protein forms a molecular complex with Hsp60 and PrPC in the human CNS, and put forth the hypothesis that this complex might become disintegrated during the conversion of PrPC into PrPSc, suggesting a mechanism for elevation of 14-3-3 in the CSF of prion diseases.

MATERIALS AND METHODS

Cell Culture

Human cell lines such as NTera2 teratocarcinoma, SK-N-S-H neuroblastoma, U-373MG astrocytoma, HeLa cervical carcinoma, and HEK293 embryonal kidney cells were obtained from the RIKEN Cell Bank (Tsukuba, Japan) and the American Type Culture Collection (Rockville, MD). They were maintained in Dulbecco's Modified Eagle's medium (DMEM; Invitrogen, Carlsbad, CA) supplemented with 10% fetal bovine serum, 100 U/mL penicillin, and 100 μg/mL streptomycin (feeding medium). For the induction of neuronal differentiation, NTera2 cells maintained in the undifferentiated state (NTera2-U) were incubated for 4 weeks in feeding medium containing 10^{-5} M *all trans*retinoic acid (Sigma, St. Louis, MO), replated twice, and then plated on a surface coated with Matrigel Basement Membrane Matrix (Becton Dickinson, Bedford, MA). They were incubated for another 2 weeks in feeding medium containing a cocktail of mitotic inhibitors, resulting in the enrichment of differentiated neurons (NTera2-N), as described previously (25).

Human neuronal progenitor (NP) cells isolated from the brain of a human fetus at 18.5 weeks' gestation were obtained from BioWhittaker (Walkersville, MD). NP cells plated on a polyethylenimine-coated surface were incubated in DMEM/F-12 medium containing an insulin–transferrin–selenium (ITS) supplement (Invitrogen), 20 ng/mL recombinant human epidermal growth factor (Higeta, Tokyo, Japan), 20 ng/mL recombinant human basic fibroblast growth factor (PeproTech EC, London, U.K.), and 10 ng/mL recombinant human leukemia inhibitory factor (Chemicon, Temecula, CA) (NP medium), as described previously (26). Reverse transcriptase–polymerase chain reaction (RT-PCR) analysis confirmed the expression of nestin mRNA, a marker for neural stem cells, in NP cells (data not shown).

Two-Dimensional Gel Electrophoresis and Mass Spectrometry Analysis

To prepare total protein extract for 2-dimensional (2D) gel electrophoretic analysis, cells and tissues were homogenized in rehydration buffer composed of 8 M urea, 2% CHAPS, 0.5% carrier ampholytes (pH 4–7 or pH 5–7), 20 mM dithiothreitol, 0.002% bromophenol blue, and a cocktail of protease inhibitors and phosphatase inhibitors (Sigma). Urea-soluble protein was separated by isoelectric focusing (IEF) using the ZOOM IPGRunner system (Invitrogen) loaded with an immobilized pH 4–7 or pH 5.3–6.3 gradient strip, according to the methods described previously (26). After the first dimension of IEF, the protein was separated in the second dimension on a NuPAGE 4% to 12% polyacrylamide gel (Invitrogen). Then, the gel was stained by the Silverquest silver staining kit (Invitrogen) or by the Pro-Q Diamond phosphoprotein gel staining kit that directly labels phosphate groups of the protein attached to serine, threonine, or tyrosine residues in the gel (Molecular Probes, Eugene, OR). For protein overlay analysis, the gel was transferred onto a polyvinylidene difluoride (PVDF) membrane. The spots of interest were excised from the gels, trypsinized, and processed for mass spectrometry (nanoESI-MS/MS) analysis followed by database searching using MASCOT software (Invitrogen Proteome, Yokohama, Japan) (26).

Protein Overlay Analysis

To prepare the probe for protein overlay, the open reading frame of the human 14-3-3ζ isoform gene or 14-3-3γ isoform gene was amplified from cDNA of NTera2-N cells by PCR using PfuTurbo DNA polymerase (Stratagene, La Jolla, CA), and sense and antisense primers listed in the Table. To prepare the full-length, N-terminal, and C-terminal fragments of HSP60 and PrPC, the human HSP60 gene or prion protein gene was amplified by PCR using a panel of primers listed in the Table. The PCR product was cloned into a prokaryotic expression vector pTrcHis-TOPO or pTrcHis2-TOPO (Invitrogen) to produce a fusion protein with an N-terminal Xpress tag or a C-terminal Myc tag. The recombinant proteins were expressed in *Escherichia coli* and purified through a HiTrap

TABLE. Primers Used for Polymerase-Chain Reaction-Based Cloning

Genes	Proteins (amino acid residues)	GenBank Accession No.	Sense Primers
YWHAZ	14-3-3ζ isoform (1–245)	NM_003406	5′atggataaaaatgagctggttcag3′
YWHAZ	14-3-3ζ isoform (1–245)	NM_003406	5′atggataaaaatgagctggttcag3′
YWHAG	14-3-3γ isoform (1–247)	NM_012479	5′atggtggaccgcgagcaactggtg3′
HSPD1	HSP60 full length (1–573)	NM_002156	5′atgcttcggttaccccacagtcttt3′
HSPD1	HSP60 N-terminal fragment (27–287)	NM_002156	5′gccaaagatgtaaaattttggtgca3′
HSPD1	HSP60 C-terminal fragment (288–573)	NM_002156	5′ttgaataggctaaaggttggtctt3′
PRNP	cellular prion protein PrPC (23–231)	NM_000311	5′aagaagcgcccgaagcctggaggatggaa3′
PRNP	PrPC N-terminal fragment (23–137)	NM_000311	5′aagaagcgcccgaagcctggaggatggaa3′
PRNP	PrPC C-terminal fragment (138–231)	NM_000311	5′atcatacatttcggcagtgactat3′

Genes	Antisense Primers	Cloning Vector
YWHAZ	5′ttaaattttccccttcttcttcctgc3′	pTrcHis-TOPO
YWHAZ	5′attttccccttcttcttcctgc3′	pTrcHis2-TOPO
YWHAG	5′ttaaattgttgccttcgccgccatc3′	pTrcHis-TOPO
HSPD1	5′ttagaacatgccacctccccatac3′	pTrcHis-TOPO
HSPD1	5′ttagacgagtgtactttagagcttc3′	pcDNA4/HisMax-TOPO
HSPD1	5′ttagaacatgccacctccccatac3′	pcDNA4/HisMax-TOPO
PRNP	5′tcagctcgatccttcttctggtaataggcctg3′	pTrcHis-TOPO
PRNP	5′tcagggcctgctcatggcacttcc3′	pcDNA4/HisMax-TOPO
PRNP	5′tcagctcgatccttcttctggtaataggcctg3′	pcDNA4/HisMax-TOPO

The PCR product was cloned into a prokaryotic expression vector pTrcHis-TOPO or pTrcHis2-TOPO to produce a fusion protein with a Xpress tag or a Myc tag in *E. coli*. It was also cloned into a mammalian expression vector pcDNA4/HisMax-TOPO to express a fusion protein with a Xpress tag in HEK293 cells.

chelating HP column (Amersham Bioscience, Piscataway, NJ) followed by separation on a SDS-PAGE gel. Recombinant human interferon-stimulated protein ISG15 (rhISG15) tagged with Xpress was prepared for a negative control probe, as described previously (26).

The PVDF membrane on which the gel was blotted was incubated at room temperature (RT) overnight with 1 μg/mL recombinant human 14-3-3ζ (rh14-3-3ζ), 14-3-3γ (rh14-3-3γ), or rhISG15, followed by immunolabeling with mouse monoclonal anti-Xpress or anti-Myc antibody (Invitrogen) and HRP-conjugated anti-mouse IgG (Santa Cruz Biotechnology, Santa Cruz, CA). After the probes and antibodies were stripped by incubating the membrane at 50°C for 30 minutes in stripping buffer composed of 62.5 mM Tris-HCl (pH 6.7), 2% SDS, and 100 mM 2-mercaptoethanol, the membrane was relabeled with goat anti-HSP60 antibody (N-20; Santa Cruz Biotechnology) followed by incubation with HRP-conjugated anti-goat IgG (Santa Cruz Biotechnology).

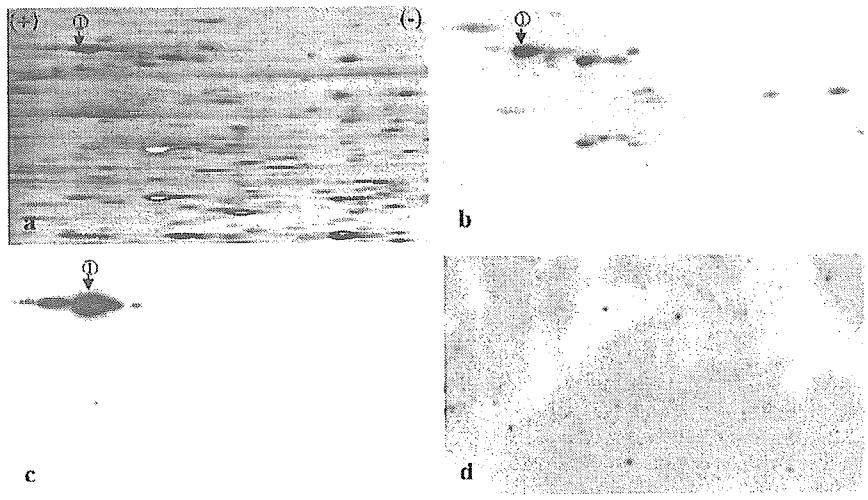

FIGURE 1. Two-dimensional gel electrophoretic analysis of 14-3-3-binding proteins in NTera2-derived differentiated neurons. Two hundred micrograms of total cellular protein isolated from NTera2-derived differentiated neurons (NTera2-N) was separated on a 2-dimensional PAGE gel (pI 5.3-6.3 for isoelectric focusing [IEF] and 4% to 12% for PAGE), silver-stained, transblotted onto a polyvinylidene difluoride (PVDF) membrane, and processed for overlay with recombinant human 14-3-3ζ protein (rh14-3-3ζ) or recombinant human interferon-stimulated protein (rhISG15) tagged with Xpress followed by labeling with anti-Xpress antibody. After the probe and antibody were stripped, the blot was relabeled with anti-Hsp60 antibody. (a) Silver staining, (b) rh14-3-3ζ, (c) Hsp60, (d) rhISG15. One major spot labeled with rh14-3-3ζ is named spot 1 (arrow).

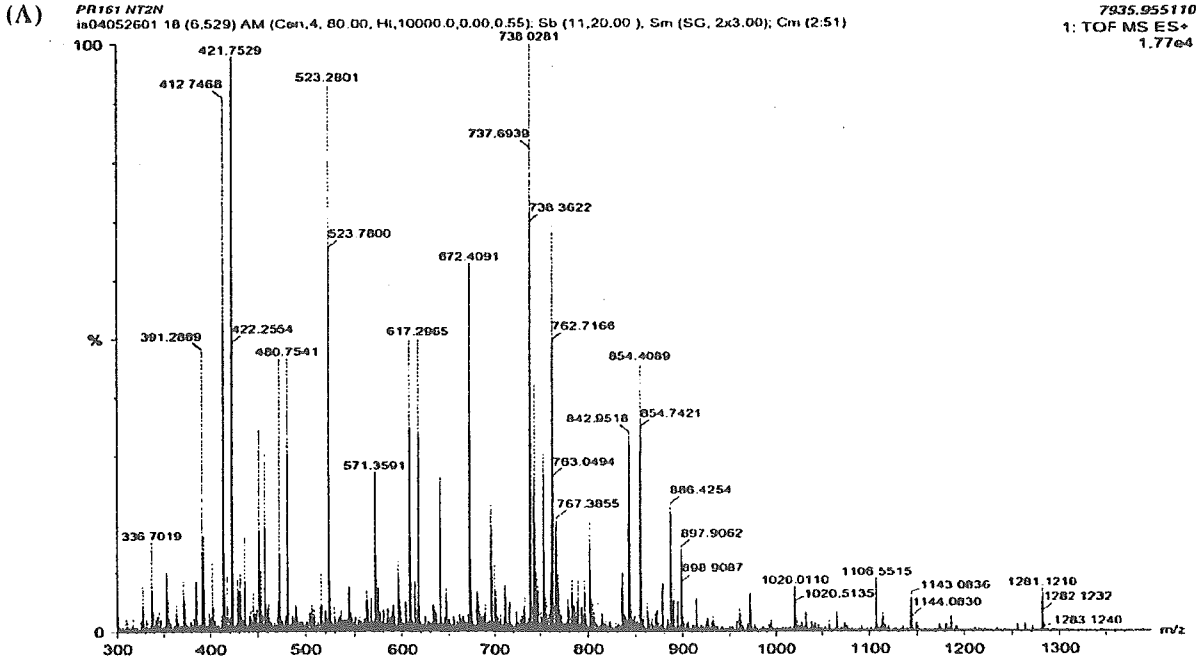

(B)

1 MLRLPTVFRQMRPVSRVLAPHLTRAYAKDVKFGADARALMLQGVDLLADAVAVTMGPKGRTVIIEQSWGSPKVTKDGVTVAKSIDLKDKYKNIGAKLVQD

101 VANNTNEEAGDGTTTATVLARSIAKEGFEKISKGANPVEIRRGVMLAVDAVIAELKKQSKPVTTPEEIAQVATISANGDKEIGNIISDAMKKVGRKGVIT

201 VKDGKTLNDELEIIEGMKFDRGYISPYFINTSKGQKCEFQDAYVLLSEKKISSIQSIVPALEIANAHRKPLVIIAEDVDGEALSTLVLNRLKVGLQVVAV

301 KAPGFGDNRKNQLKDMAIATGGAVFGEEGLTLNLEDVQPHDLGKVGEVIVTKDDAMLLKGKGDKAQIEKRIQEIIEQLDVTTSEYEKEKLNERLAKLSDG

401 VAVLKVGGTSDVEVNEKKDRVTDALNATRAAVEEGIVLGGGCALLRCIPALDSLTPANEDQKIGIEIIKRTLKIPAMTIAKNAGVEGSLIVEKIMQSSSE

501 VGYDAMAGDFVNMVEKGIIDPTKVVRTALLDAAGVASLLTTAEVVVTEIPKEEKDPGMGAMGGMGGGMGGGMF

FIGURE 2. Mass spectrometric analysis of the 14-3-3-binding protein in NTera2-N cells. Spot 1 labeled with the rh14-3-3ζ probe (Fig. 1) was excised from the gel, trypsinized, and processed for nanoESI-MS/MS analysis. (A) The spectra of MS analysis. Each peak indicates individual peptide fragments. The positions of several peaks were automatically numbered on the spectra. The fragments were selected for MS analysis in order of their signal intensity, although autolytic fragments of trypsin (e.g. 412, 421, 523, 737, 762, and 767) were omitted. (B) Amino acid sequence of human Hsp60. Seventeen peptide fragments of spot 1 identified by MS analysis (shadowed) showed a perfect match with the sequence encompassing amino acid residues 38–493 of human Hsp60. The number indicated on each fragment represents the position in the horizontal axis of the spectra.

Immunoprecipitation Analysis

To express recombinant human proteins in cultured cells, the PCR product was cloned into a mammalian expression vector pcDNA4/HisMax-TOPO (Invitrogen) to produce a fusion protein with an N-terminal Xpress tag. The vector was transfected in HEK293 cells by Lipofectamine 2000 reagent (Invitrogen).

To prepare total protein extract for immunoprecipitation (IP) analysis, cells and tissues were homogenized in M-PER lysis buffer (Pierce, Rockford, IL) with a cocktail of protease inhibitors and phosphatase inhibitors (Sigma) followed by centrifugation at 12,000 rpm at 4°C for 20 minutes. After preclearance, the supernatant was incubated at 4°C for 3 hours with 30 μg/mL rabbit polyclonal anti-14-3-3 protein antibody (K19)-conjugated agarose (Santa Cruz Biotechnology) or the same amount of normal rabbit IgG-conjugated agarose (Santa Cruz Biotechnology). After several washes, the immunoprecipitates were processed for Western blot analysis using anti-HSP60 antibody (N-20), mouse monoclonal, anti-prion protein antibody (3F4; Dako, Carpinteria, CA), mouse monoclonal anti-14-3-3 protein antibody (H-8; Santa Cruz Biotechnology), or anti-Xpress antibody.

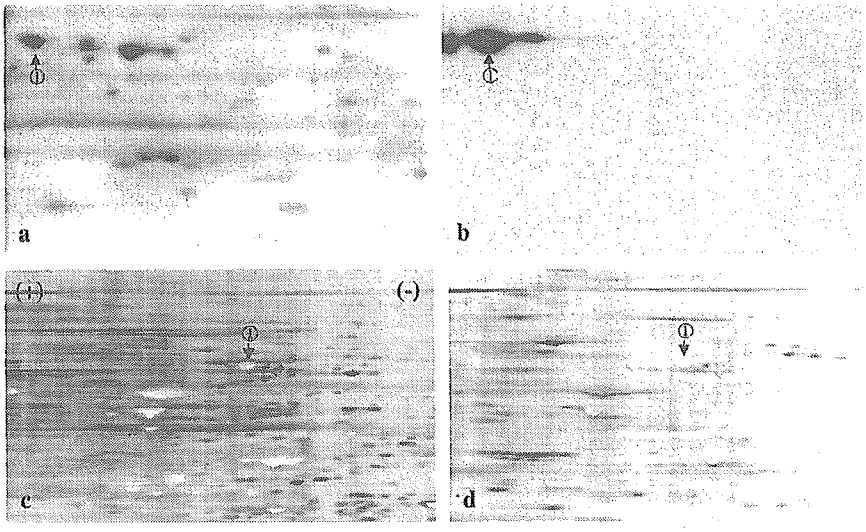

FIGURE 3. The interaction of 14-3-3 protein with Hsp60 was not zeta isoform-specific. Two hundred micrograms of total cellular protein of NTera2-N was separated on a 2-dimensional PAGE gel ([a, b]: pI 5.3–6.3 and 4%–12%; [c, d]: pI 4–7 and 4%–12%), followed by silver staining or phosphoprotein staining. The gel was processed for overlay with recombinant human 14-3-3γ protein (rh14-3-3γ) tagged with Xpress, followed by relabeling with anti-Hsp60 antibody. (a) rh14-3-3ζ, (b) Hsp60, (c) silver staining, (d) phosphoprotein staining. Spot 1 is indicated by an arrow.

Immunocytochemistry and Immunohistochemistry

For double-labeling immunocytochemistry, cells plated on cover glasses were fixed with 4% paraformaldehyde in 0.1 M phosphate buffer (pH 7.4) at RT for 10 minutes followed by incubation with phosphate-buffered saline (PBS) containing 0.5% Triton X-100 at RT for 20 minutes and with PBS containing 10% normal human serum at RT for 15 minutes. In some experiments, live cells were labeled with MitoTracker Red CMXRos (Molecular Probes) before fixation. The cells were then incubated at RT for 30 minutes with anti-HSP60 antibody (N-20) followed by incubation with Rhodamine Red-X-conjugated anti-goat IgG (Jackson ImmunoResearch, West Grove, PA). They were then incubated with rabbit anti-14-3-3ζ isoform antibody (IBL, Gumma, Japan) or mouse monoclonal anti-prion protein antibody (8G8; Cayman Chemical, Ann Arbor, MI) followed by incubation with Alexa Fluor 488-conjugated anti-rabbit or anti-mouse IgG (Molecular Probes). In limited experiments, the cells were incubated at RT for 5 minutes with 4′,6′-diamidino-2-phenylindole (DAPI) (1:30,000; Molecular Probes). After several washes, cover glasses were mounted on the slides with glycerol–polyvinyl alcohol and examined under a Nikon ECLIPSE E800 universal microscope. Negative controls were processed following these steps except for exposure to primary antibody.

For immunohistochemistry, 10-μm-thick serial sections were prepared from several autopsy brains of multiple sclerosis and cerebral infarction. Detailed clinical profiles of the patients were described previously (26). The brains were fixed with 4% paraformaldehyde and embedded in paraffin. After deparaffination, the tissue sections were heated by microwave at 95°C for 10 minutes in 10 mM citrate sodium buffer (pH 6.0) followed by incubation at RT for 15 minutes with 3% H_2O_2-containing methanol. For prion protein immunolabeling, the sections were pretreated by boiling for 20 minutes in the citrate sodium buffer according to the methods described previously (27). The tissue sections were then incubated with PBS containing 10% normal goat or rabbit serum at RT for 15 minutes to block nonspecific staining. They were then incubated at 4°C overnight with anti-14-3-3ζ isoform antibody (IBL), anti-HSP60 antibody (N-20), anti-prion protein antibody (8G8), rabbit anti-glial fibrillary acidic protein (GFAP) antibody (N1506; Dako), or rabbit anti-neuron-specific enolase (NSE) antibody (Nichirei, Tokyo, Japan). After washing with PBS, the tissue sections were labeled at RT for 30 minutes with peroxidase-conjugated secondary antibodies (Simple Stain MAX-PO kit, Nichirei) followed by incubation with a colorizing solution containing diaminobenzidine tetrahydrochloride (DAB) and a counterstain with hematoxylin. For negative controls, the sections were incubated with a negative control reagent (Dako) instead of primary antibodies.

RESULTS

Identification of Hsp60 as a 14-3-3-Binding Protein in Human Neurons

To identify 14-3-3-binding proteins in human neurons, we performed a protein overlay analysis using recombinant human 14-3-3ζ protein (rh14-3-3ζ) tagged with Xpress as a probe. Total protein extract of NTera2-derived differentiated neurons (NTera2-N) was separated on a 2D-PAGE gel and transferred onto a PVDF membrane (Fig. 1). The rh14-3-3ζ probe reacted strongly with several spots on the blot, among which a major 60-kDa spot was designated spot 1 (Fig. 1b). In contrast, the rhISG15 probe did not label any of these spots, excluding nonspecific binding of rh14-3-3ζ through the Xpress tag (Fig. 1d). Spot 1 was excised from the original gel, trypsinized, and processed for nanoESI-MS/MS analysis (Fig. 2A). Seventeen peptide fragments derived from the spot 1 showed a perfect match with the sequence covering amino acid residues 38–493 of human Hsp60 (Fig. 2B). This indicates that spot 1 corresponds to the nearly full length of Hsp60. Anti-Hsp60 antibody labeled spot 1, verifying the results (Fig. 1c). Furthermore, the rh14-3-3γ probe also

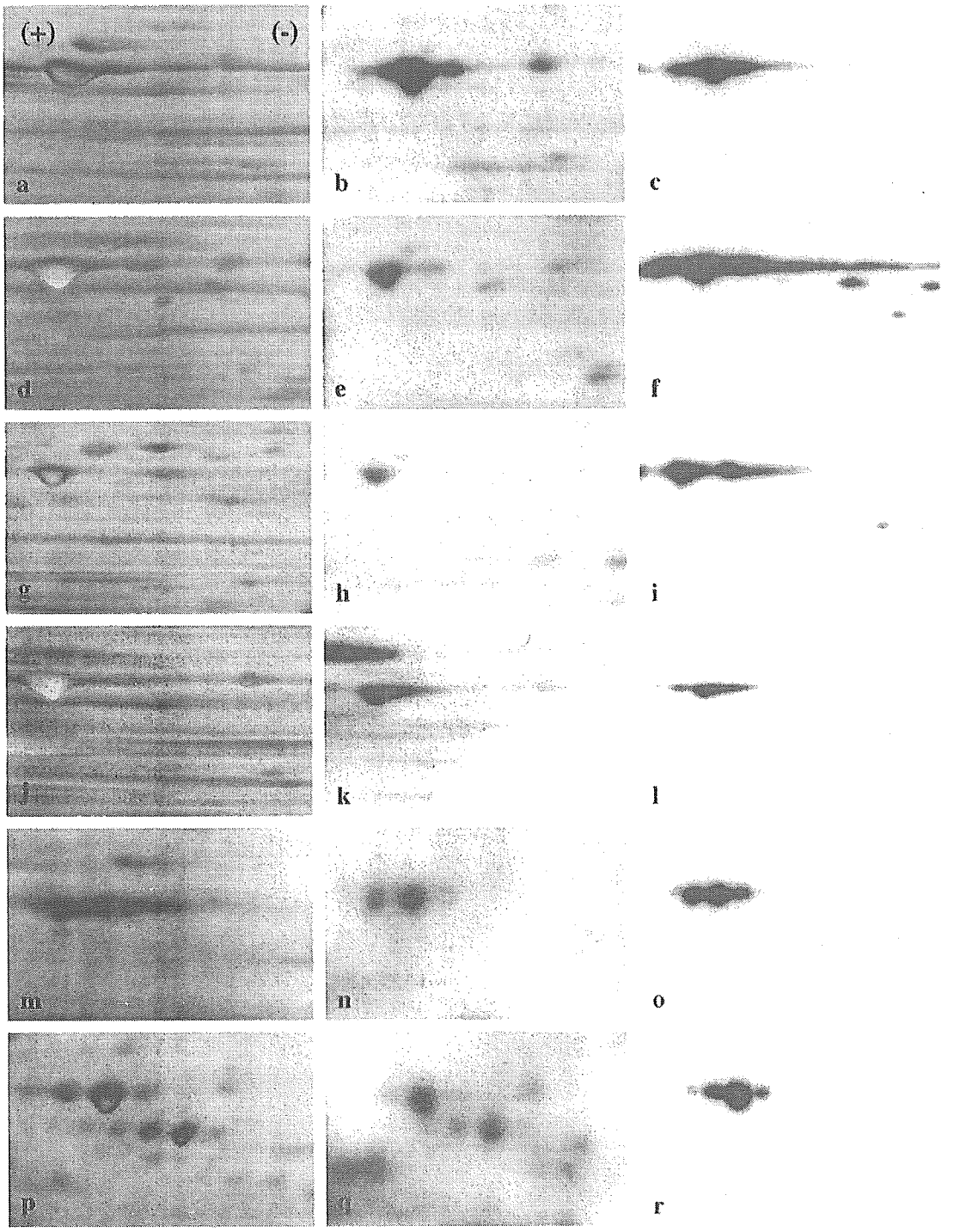

FIGURE 4. The interaction of 14-3-3 protein with Hsp60 was universal in neuronal and nonneuronal cells. Two hundred micrograms of total cellular protein of human cell lines and brain homogenate was separated on a 2-dimensional PAGE gel ([**a–l**]: pI 5.3–6.3 and 4% to 12%; [**m–r**]: pI 4-7 and 4% to 12%) followed by silver staining (the left panels). The gel was processed for overlay with the rh14-3-3ζ probe tagged with Xpress or Myc (the center panels) followed by relabeling with anti-Hsp60 antibody (the right panels). (**a–c**) Undifferentiated NTera2 teratocarcinoma (NTera2-U), (**d–f**) SK-N-SH neuroblastoma, (**g–i**) U-373MG astrocytoma, (**j–l**) HeLa cervical carcinoma, (**m–o**) human neuronal progenitor (NP) cells, (**p–r**) brain homogenate.

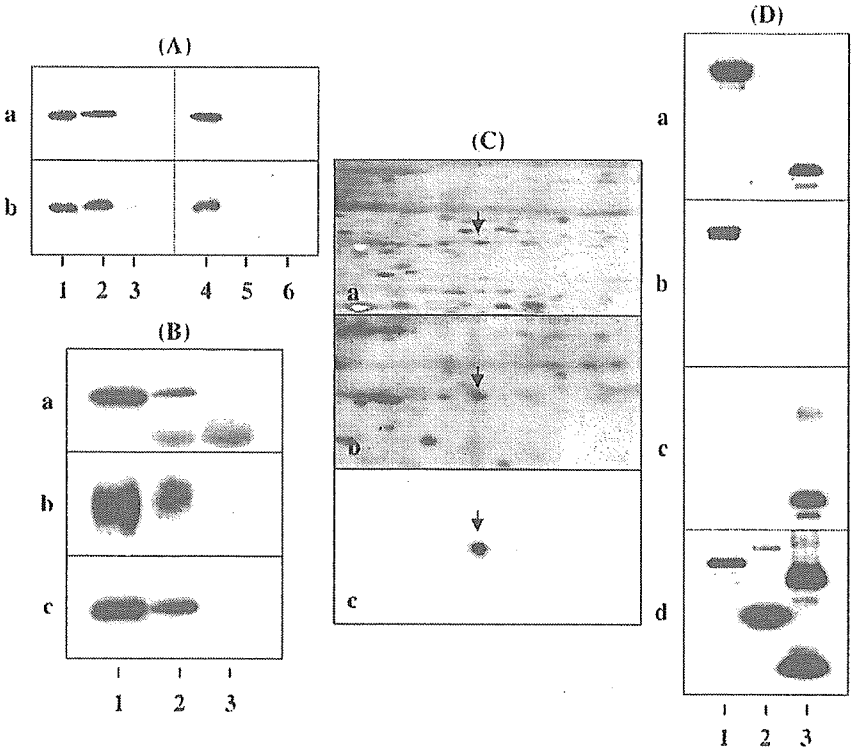

FIGURE 5. The interaction of 14-3-3 protein with both Hsp60 and PrPC. **(A)** The 14-3-3-binding domains of Hsp60 and PrPC. Either the N-terminal half (NTF) (lanes 1–3) or the C-terminal half (CTF) (lanes 4–6) of (a) recombinant human HSP60 or (b) PrPC tagged with Xpress was separately expressed in HEK293 cells. The cellular protein extract was processed for immunoprecipitation (IP) with (2, 5) anti-14-3-3 protein antibody (K-19) or (3, 6) rabbit IgG, followed by immunoblotting with anti-Xpress antibody. The lanes (1, 4) indicate the input control. **(B)** Coimmunoprecipitation of 14-3-3 with Hsp60 and PrPC. Human brain homogenate was processed for IP with (2) K-19 or (3) rabbit IgG followed by immunoblotting with (a) anti-Hsp60 antibody (N-20), (b) anti-prion protein antibody (3F4), or (c) anti-14-3-3 protein antibody (H8). Lane (1) indicates the input control. **(C)** The interaction of 14-3-3 with PrPC. Two hundred micrograms of human brain protein extract was separated on a 2-dimensional PAGE gel (pI 4–7 and 4%–12%), silver-stained, and processed for overlay with the rh14-3-3ζ probe tagged with Myc followed by relabeling with anti-prion protein antibody (3F4). (a) Silver staining, (b) rh14-3-3ζ, (c) PrPC. **(D)** Phosphorylation-independent interaction of 14-3-3 with Hsp60 and PrPC. Xpress-tagged recombinant proteins of (1) human Hsp60, (2) LacZ fragment, and (3) human PrPC produced by *Escherichia coli* were processed for overlay with (a) the rh14-3-3ζ probe tagged with Myc, followed by relabeling with (b) anti-Hsp60 antibody (N-20), (c) anti-prion protein antibody (3F4), or (d) anti-Xpress antibody.

reacted with spot 1, suggesting that the interaction of 14-3-3 with Hsp60 is not ζ isoform-specific (Fig. 3a, b). Hsp60 does not possess a substantial amount of phosphorylated amino acid residues, because spot 1 was not labeled by the phosphoprotein gel stain (Fig. 3c, d).

To study whether the interaction of 14-3-3 with Hsp60 is a neuron-specific event, protein extracts of undifferentiated NTera2 (NTera2-U), SK-N-SH neuroblastoma, U-373MG astrocytoma, HeLa cervical carcinoma, human NP cells, and human brain homogenate were separated on a 2D-PAGE gel and processed for protein overlay with the rh14-3-3ζ probe tagged with Xpress or Myc. This identified Hsp60 as a universal binding partner for the 14-3-3 protein (Fig. 4a–r).

The 14-3-3-Interacting Domain Was Located in N-Terminal Half of Hsp60

To identify the 14-3-3-binding site of Hsp60, either the N-terminal half with cleavage of the mitochondrial import signal (NTF; amino acid residues 27–287) or the C-terminal half (CTF; amino acid residues 288–573) of human Hsp60 was separately expressed in HEK293 cells. Then, total cellular protein was processed for immunoprecipitation (IP) with anti-14-3-3 protein antibody. The NTF but not CTF of Hsp60 was coimmunoprecipitated, indicating that the 14-3-3-interacting domain is located in the NTF of Hsp60 (Fig. 5A, panel a).

Phosphorylation-Independent Interaction of 14-3-3 Protein With Hsp60 and PrPC

By IP of human brain protein with anti-14-3-3 protein antibody, cellular prion protein (PrPC) along with Hsp60 was coimmunoprecipitated with 14-3-3 (Fig. 5B, panels a–c). In contrast, Raf-1, one of the well-known 14-3-3-binding partners, was not coimmunoprecipitated with 14-3-3 in the human brain homogenate (data not shown). By protein overlay of human brain homogenate, the rh14-3-3ζ probe reacted with PrPC, suggesting that PrPC is another 14-3-3 protein-interacting protein (Fig. 5C, panels a–c). Furthermore, the rh14-3-3ζ probe labeled both recombinant human Hsp60 (66 kDa) and PrPC (32 kDa), but did not label a LacZ fragment (44 kDa), all of which were produced by *E. coli* as non-phosphorylated forms tagged with Xpress (Fig. 5D, panels a–d). This indicates that the molecular interaction of 14-3-3 with Hsp60 and PrPC is direct but phosphorylation-independent. To identify the 14-3-3-binding site of PrPC, either the NTF (amino acid residues 23–137) or the CTF (amino acid residues 138–231) of human PrPC was separately expressed in HEK293 cells. Then, total cellular protein was processed

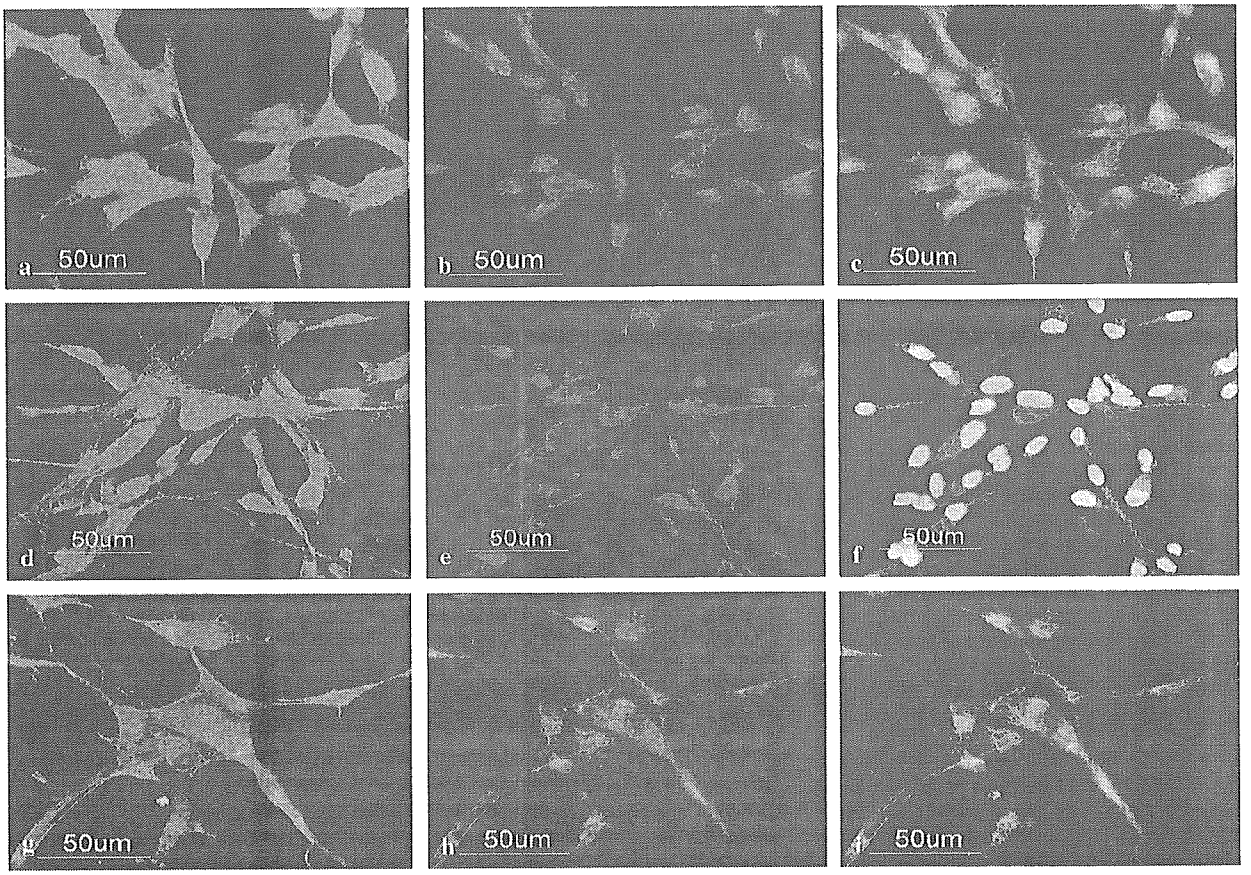

FIGURE 6. Colocalization of 14-3-3 protein, Hsp60, and PrPC in the mitochondria of human neuronal progenitor cells. Human neuronal progenitor (NP) cells were immunolabeled with 14-3-3ζ isoform-specific antibody, anti-Hsp60 antibody, anti-prion protein antibody (8G8), MitoTracker Red CMXRos, or DAPI followed by staining with secondary antibodies. **(a)** 14-3-3ζ, **(b)** Hsp60, **(c)** merge of **(a)** and **(b)**; **(d)** 14-3-3ζ, **(e)** CMXRos, **(f)** merge of **(d)** and **(e)** labeled with DAPI; **(g)** PrPC, **(h)** Hsp60, **(i)** merge of **(g)** and **(h)**.

for IP with anti-14-3-3 protein antibody. The NTF but not CTF of PrPC was coimmunoprecipitated, indicating that the 14-3-3-interacting domain is located in the NTF of PrPC (Fig. 5A, panel b).

Coexpression of 14-3-3 Protein, Hsp60, and PrPC in Vitro and in Vivo

To determine whether 14-3-3, Hsp60, and PrPC are colocalized in the same subcellular compartment, cultured human NP cells were double-immunolabeled with the 14-3-3ζ isoform-specific antibody, anti-Hsp60 antibody, and anti-prion protein antibody. An intense immunoreactivity for 14-3-3 was located chiefly in the cytoplasm, and less abundantly in the nucleus and the plasma membrane, whereas Hsp60 immunolabeling was found almost exclusively in the cytoplasm (Fig. 6a, b). Hsp60 showed a granular distribution pattern identical to the location of the mitochondria, where both 14-3-3 and Hsp60 were found to be colocalized (Fig. 6c). A considerable overlap was found between the 14-3-3 immunoreactivity and the staining of a mitochondrial dye, being devoid of the nucleus (Fig. 6d–f). Furthermore, PrPC was colocalized with Hsp60 (Fig. 6g–i). These results indicate that the 14-3-3 protein, Hsp60, and PrPC are colocalized chiefly in the mitochondria of human neuronal progenitor cells in culture, although an extramitochondrial coexpression of these proteins at very low levels could not be excluded.

In the human brain sections, nearly all of NSE^+ cortical neurons and $GFAP^+$ reactive astrocytes showed an intense cytoplasmic immunoreactivity for 14-3-3, Hsp60 and PrPC, suggesting that these three proteins are coexpressed most prominently in neurons (Fig. 7a–d) and reactive astrocytes (Fig. 8a–d) and to a lessor degree in microglia/macrophages (not shown) in the human CNS in vivo.

DISCUSSION

The present study, by protein overlay, mass spectrometry, and immunoprecipitation analysis, identified Hsp60 and PrPC as 14-3-3-interacting proteins. PrPC along with Hsp60 was coimmunoprecipitated with 14-3-3 from the human brain homogenate. The 14-3-3-binding domain is located in the NTF

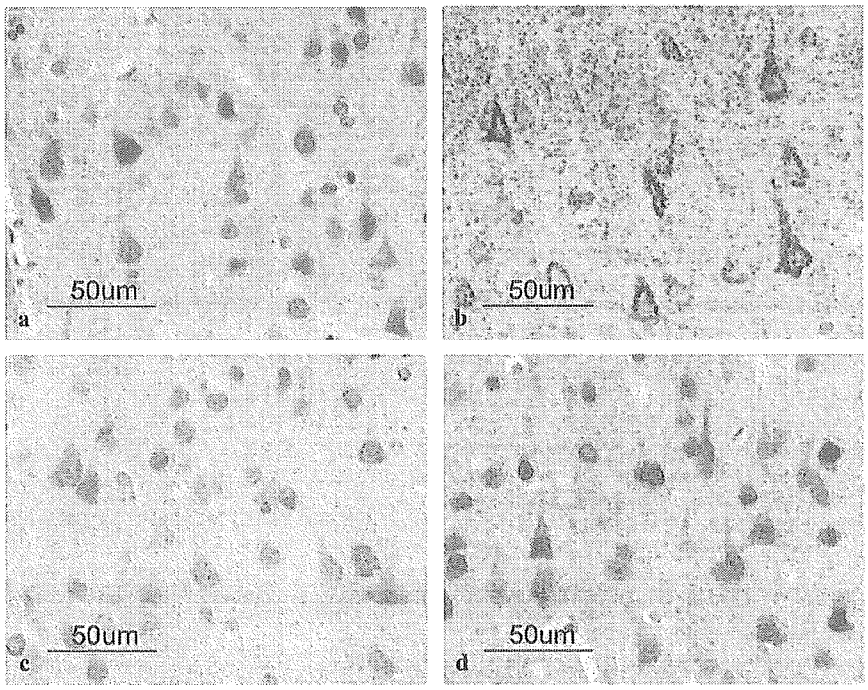

FIGURE 7. Coexpression of 14-3-3 protein, Hsp60, and PrPC in neurons in the human brain. Serial sections derived from autopsied brains of multiple sclerosis were processed for immunohistochemistry using 14-3-3ζ isoform-specific antibody, anti-Hsp60 antibody, anti-prion protein antibody (8G8), or anti-neuron-specific enolase (NSE) antibody. (a–d) The cerebral cortex of the frontal lobe of #791 MS: (a) 14-3-3ζ, (b) Hsp60, (c) PrPC, (d) NSE.

of Hsp60 and the NTF of PrPC in HEK293 cells over-expressing the transgenes. The 14-3-3 protein, Hsp60, and PrPC were colocalized chiefly in the mitochondria of human NP cells in culture, and they were coexpressed most obviously in neurons and reactive astrocytes in the human brain by immunohistochemistry. The interaction of 14-3-3 with Hsp60 and PrPC was phosphorylation-independent, because Hsp60 was found to be not substantially phosphorylated by the phosphoprotein gel stain, and the 14-3-3 probe reacted with nonphosphorylated forms of recombinant Hsp60 and PrPC by

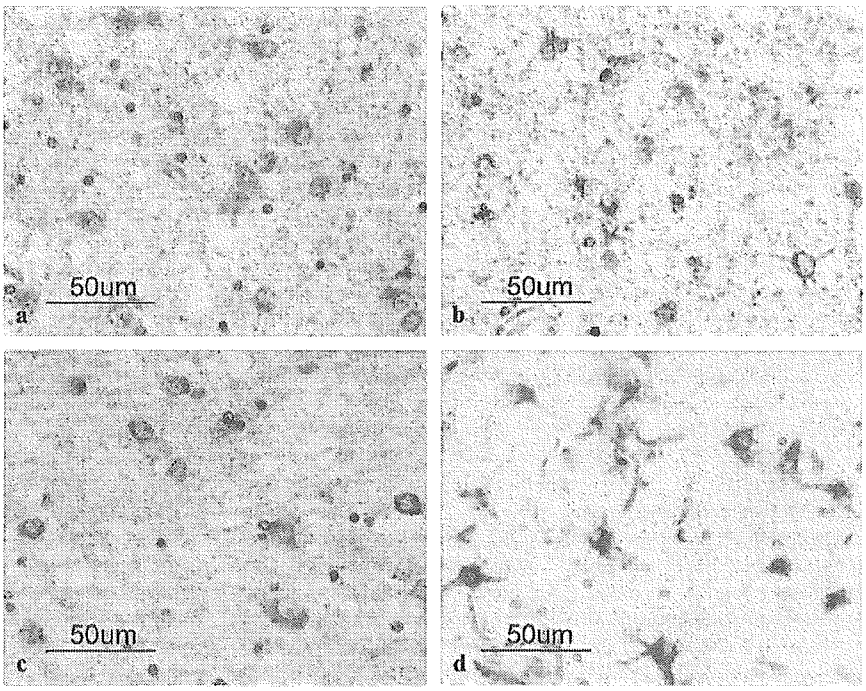

FIGURE 8. Coexpression of 14-3-3 protein, Hsp60, and PrPC in reactive astrocytes in the human brain. Serial sections derived from autopsied brains of multiple sclerosis were processed for immunohistochemistry using 14-3-3ζ isoform-specific antibody, anti-Hsp60 antibody, anti-prion protein antibody (8G8), or anti-GFAP antibody. (a–d) Chronic active demyelinating lesions in the subcortical white matter of the frontal lobe of 744 multiple sclerosis: (a) 14-3-3ζ, (b) Hsp60, (c) PrPC, (d) GFAP.

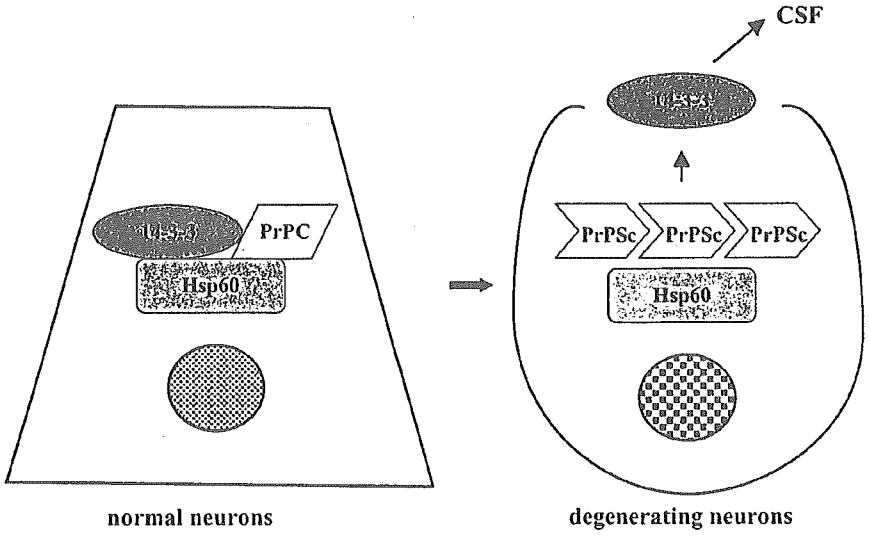

FIGURE 9. A possible mechanism for elevation of 14-3-3 protein in the cerebrospinal fluid of prion diseases. When affected with the pathogenetic prion, the molecular complex composed of 14-3-3, Hsp60, and PrPC becomes disintegrated during the conversion of PrPC into PrPSc aggregates, which displace the 14-3-3 protein from the complex, resulting in the release of 14-3-3 from degenerating neurons into the cerebrospinal fluid.

protein overlay analysis. These observations indicate that the 14-3-3 protein forms a molecular complex with Hsp60 and PrPC in the human CNS.

PrPC is a glycosylphosphatidylinositol (GPI) anchored cell-surface protein, expressed at highest levels in neurons and at substantial levels in astrocytes in the CNS (28, 29). Although a low level of extramitochondrial coexpression could not be excluded, the present study showed the substantial colocalization of 14-3-3, Hsp60, and PrPC in the mitochondria of human NP cells, not in agreement with the predominant location of PrPC on the cell surface. However, several recent studies showed that defined populations of neurons express PrPC in the cytoplasm as well as on the plasma membrane (27, 30). PrPC interacts with the C-terminus of Bcl-2 in the mitochondrial transmembrane region (31), and transgenic mice overexpressing wild-type PrPC show the expression of PrPC in the mitochondria (32), suggesting that the mitochondrial location of PrPC in cultured human NP cells does not seem unlikely. Increasing evidence suggests that the conformational conversion of α-helix-rich PrPC into β-sheet-rich PrPSc involves a molecular chaperone-like factor. A previous study using a yeast 2-hybrid system showed that Hsp60 interacts with PrPC, where the docking site was mapped between amino acid residues 180 and 210 of PrPC (33). GroEL, a homolog of eukaryotic Hsp60, mediates the aggregation of recombinant PrPC and promotes the conversion of PrPC into PrPSc in an ATP-dependent manner (23, 24). Furthermore, Hsp60 of the *Brucella abortus* directly binds PrPC of the host macrophages, and this binding promotes the aggregation of PrPC on the cell-surface lipid rafts (34). Interestingly, circulating antibodies against *Spiroplasma* Hsp60 were detected exclusively in patients with CJD, suggesting that the bacterial Hsp60, highly homologous to the host Hsp60, might play an active role in the pathologic process of prion diseases (35). Heat shock elements were identified in the promoter region of prion protein gene (36). PrPC exhibits an antioxidant activity (37), and stress-inducing stimuli such as reactive oxygen species, heat shock, and proinflammatory cytokines elevate the levels of PrPC expression in cultured cells (36, 38, 39). These observations suggest that PrPC and endogenous cellular Hsp are coordinately upregulated in certain cell types under pathologic conditions.

Supporting the present observations, several recent studies identified Hsp60 as one of 14-3-3-interacting proteins in HeLa and HEK293 cells by immunoaffinity purification (9, 40, 41). Hsp60 constitutes a heptameric cylindrical complex composed of identical subunits stacked back to back, forming a double-ring structure. The Anfinsen cage of Hsp60 contains a central cavity where substrate proteins are sequestered and properly folded in cooperation with the Hsp10 family protein (19, 20). In addition, several proteins that are too large to fit the cage are processed for chaperoning outside the cage (42). Hsp60 is located primarily in the mitochondrial matrix, where it mediates the folding of newly imported mitochondrial matrix proteins and the assembly of large multiprotein complexes (43). Importantly, the 14-3-3 protein that does not have a mitochondrial targeting signal is also identified within the mitochondria (44). A recent study showed that an exposure to cisplatin upregulates simultaneously Hsp60 and 14-3-3 expression in human squamous cell carcinoma (45). Kinase suppressor of Ras (KSR), a regulator of the Ras-MAP kinase pathway, forms a multimolecular signaling complex composed of Hsp90, Hsp70, Hsp68, $p50^{CDC37}$, MEK1, MEK2, and 14-3-3 proteins, where a panel of Hsp serve to stabilize KSR (46). It is worthy to note that the levels of expression of the cytosolic chaperonin CCT6A are reduced in the brain of 14-3-3γ isoform-knockout mice, although these mice show a clinical course similar to the wild-type mice after inoculation of scrapie prion (47). Because the 14-3-3 protein acts as an allosteric regulator that stabilizes the binding partners in a particular conformation (3, 4), we could suggest the following scenario (Fig. 9). The interaction of 14-3-3 with PrPC might prevent PrPC from the autocatalytic conformational change under physiological conditions. When affected with the pathogenetic prion, PrPSc aggregates displace 14-3-3

protein from the molecular complex during the conversion of PrPC into PrPSc that is promoted by Hsp60, resulting in the release of 14-3-3 from degenerating neurons into the CSF.

ACKNOWLEDGMENTS

The authors thank Dr. Masashi Fukuda, Invitrogen Proteome, Yokohama, Japan, for his help in nanoESI-MS/MS analysis; and Ms. Chizuru Soma and Ms. Ayako Sakamoto, NCNP, Tokyo, Japan, for their technical assistance. All autopsied brain samples were obtained from the Research Resource Network (RRN), Japan.

REFERENCES

1. Fu H, Subramanian RR, Masters SC. 14-3-3 proteins: Structure, function, and regulation. Annu Rev Pharmacol Toxicol 2000;40:617–47
2. van Hemert MJ, Steensma HY, van Heusden GPH. 14-3-3 proteins: Key regulators of cell division, signaling and apoptosis. Bioessays 2001; 23:936–47
3. Dougherty MK, Morrison DK. Unlocking the code of 14-3-3. J Cell Sci 2004;117:1875–84
4. MacKintosh C. Dynamic interactions between 14-3-3 proteins and phosphoproteins regulate diverse cellular processes. Biochem J 2004;381: 329–42
5. Berg D, Holzmann C, Riess O. 14-3-3 proteins in the nervous system. Nature Rev Neurosci 2002;4:752–62
6. Ostrerova N, Petrucelli L, Farrer M, et al. α-Synuclein shares physical and functional homology with 14-3-3 proteins. J Neurosci 1999;19:5782–91
7. Agarwal-Mawal A, Qureshi HY, Cafferty PW, et al. 14-3-3 connects glycogen synthase kinase-3β to tau within a brain microtubule-associated tau phosphorylation complex. J Biol Chem 2003;278:12722–28
8. Chen H-K, Fernandez-Funez P, Acevedo SF, et al. Interaction of Akt-phosphorylated ataxin-1 with 14-3-3 mediates neurodegeneration in spinocerebellar ataxia type 1. Cell 2003;113:457–68
9. Meek SEM, Lane WS, Piwnica-Worms H. Comprehensive proteomic analysis of interphase and mitotic 14-3-3-binding proteins. J Biol Chem 2004;279:32046–46
10. Zhai J, Lin H, Shamim M, et al. Identification of a novel interaction of 14-3-3 with p190RhoGEF. J Biol Chem 2001;276:41318–24
11. Henriksson ML, Francis MS, Peden A, et al. A nonphosphorylated 14-3-3 binding motif on exoenzyme S that is functional in vivo. Eur J Biochem 2002;269:4921–29
12. Dai J-G, Murakami K. Constitutively and autonomously active protein kinase C associated with 14-3-3 ζ in the rodent brain. J Neurochem 2003;84:23–34
13. Yuan H, Michelsen K, Schwappach B. 14-3-3 dimers probe the assembly status of multimeric membrane proteins. Curr Biol 2003;13:638–46
14. Hsich G, Kenney K, Gibbs CJ Jr., et al. The 14-3-3 brain protein in cerebrospinal fluid as a marker for transmissible spongiform encephalopathies. N Engl J Med 1996;335:924–30
15. Zerr I, Bodemer M, Gefeller O, et al. Detection of 14-3-3 protein in the cerebrospinal fluid supports the diagnosis of Creutzfeldt-Jakob disease. Ann Neurol 1998;43:32–40
16. Richard M, Biacabe A-G, Streichenberger N, et al. Immunohistochemical localization of 14.3.3 ζ protein in amyloid plaques in human spongiform encephalopathies. Acta Neuropathol 2003;105:296–302
17. Prusiner SB. Prions. Proc Natl Acad Sci U S A 1998;95:13363–83
18. Hartl FU, Mayer-Hartl M. Molecular chaperones in the cytosol: From nascent chain to folded protein. Science 2002;295:1852–58
19. Bukau B, Horwich AL. The Hsp70 and Hsp60 chaperone machines. Cell 1998;92:351–66
20. Richardson A, Landry SJ, Georgopoulos C. The ins and outs of a molecular chaperone machine. Trends Biochem Sci 1998;23:138–43
21. Muchowski PJ, Wacker JL. Modulation of neurodegeneration by molecular chaperones. Nature Rev Neurosci 2005;6:11–22
22. Hansen JJ, Dürr A, Cournu-Rebeix I, et al. Hereditary spastic paraplegia SPG13 is associated with a mutation in the gene encoding the mitochondrial chaperonin Hsp60. Am J Hum Genet 2002;70:1328–32
23. DebBurman SK, Raymond GJ, Caughey B, et al. Chaperone-supervised conversion of prion protein to its protease-resistant form. Proc Natl Acad Sci U S A 1997;94:13938–43
24. Stöckel J, Hartl FU. Chaperonin-mediated de novo generation of prion protein aggregates. J Mol Biol 2001;313:861–72
25. Satoh J-I, Kuroda Y. Differential gene expression between human neurons and neuronal progenitor cells in culture: An analysis of arrayed cDNA clones in NTera2 human embryonal carcinoma cell line as a model system. J Neurosci Methods 2000;94:155–64
26. Satoh J-I, Yamamura T, Arima K. The 14-3-3 protein ε isoform expressed in reactive astrocytes in demyelinating lesions of multiple sclerosis binds to vimentin and glial fibrillary acidic protein in cultured human astrocytes. Am J Pathol 2004;165:577–92
27. Kovacs GG, Voigtländer T, Hainfellner JA, et al. Distribution of intraneuronal immunoreactivity for the prion protein in human prion diseases. Acta Neuropathol 2002;104:320–26
28. Bendheim PE, Brown HR, Rudelli RD, et al. Nearly ubiquitous tissue distribution of the scrapie agent precursor protein. Neurology 1992;42: 149–56
29. Moser M, Colello RJ, Pott U, et al. Developmental expression of the prion protein gene in glial cells. Neuron 1995;14:509–17
30. Mironov A Jr, Latawiec D, Wille H, et al. Cytosolic prion protein in neurons. J Neurosci 2003;23:7183–93
31. Kurschner C, Morgan JI. Analysis of interaction sites in homo-and heteromeric complexes containing Bcl-2 family members and the cellular prion protein. Mol Brain Res 1996;37:249–58
32. Hachiya NS, Yamada M, Watanabe K, et al. Mitochondrial localization of cellular prion protein (PrP^C) invokes neuronal apoptosis in aged transgenic mice overexpressing PrP^C. Neurosci Lett 2005;374:98–103
33. Edenhofer F, Rieger R, Famulok M, et al. Prion protein PrP^C interacts with molecular chaperones of the Hsp60 family. J Virol 1996;70: 4724–28
34. Watarai M, Kim S, Erdenebaatar J, et al. Cellular prion protein promotes *Brucella* infection into macrophages. J Exp Med 2003;198:5–17
35. Moyer P. Spiroplasma Hsp60 may be the pathogen responsible for spreading CJD. Neurol Today 2004;4:8–11
36. Shyu W-C, Ham H-J, Saeki K, et al. Molecular modulation of expression of prion protein by heat shock. Mol Neurobiol 2002;26:1–12
37. White AR, Collins SJ, Maher F, et al. Prion protein-deficient neurons reveal lower glutathione reductase activity and increased susceptibility to hydrogen peroxide toxicity. Am J Pathol 1999;155:1723–30
38. Satoh J-I, Kurohara K, Yukitake M, et al. Constitutive and cytokine-inducible expression of prion protein gene in human neural cell lines. J Neuropathol Exp Neurol 1998;57:131–39
39. Sauer H, Dagdanova A, Hescheler J, et al. Redox-regulation of intrinsic prion expression in multicellular prostate tumor sheroids. Free Radic Biol Med 1999;27:1276–83
40. Jin J, Smith FD, Stark C, et al. Proteomic, functional, and domain-based analysis of in vivo 14-3-3 binding proteins involved in cytoskeletal regulation and cellular organization. Curr Biol 2004;14: 1436–50
41. Pozuelo Rubio M, Geraghty KM, Wong BHC, et al. 14-3-3-affinity purification of over 200 human phosphoproteins reveals new links to regulation of cellular metabolism, proliferation and trafficking. Biochem J 2004;379:395–408
42. Chaudhuri TK, Farr GW, Fenton WA, et al. GroEL/GroES-mediated folding of a protein too large to be encapsulated. Cell 2001;107:235–46
43. Cheng MY, Hartl FU, Martin J, et al. Mitochondrial heat-shock protein hsp60 is essential for assembly of proteins imported into yeast mitochondria. Nature 1989;337:620–25
44. Pierrat B, Ito M, Hinz W, et al. Uncoupling proteins 2 and 3 interact with members of the 14.3.3 family. Eur J Biochem 2000;267:2680–87
45. Castagna A, Antonioli P, Astner H, et al. A proteomic approach to cisplatin resistance in the cervix squamous cell carcinoma cell line A431. Proteomics 2004;4:3246–67
46. Stewart S, Sundaram M, Zhang Y, et al. Kinase suppressor of Ras forms a multiprotein signaling complex and modulates MEK localization. Mol Cell Biol 1999;19:5523–34
47. Steinacker P, Schwarz P, Reim K, et al. Unchanged survival rates of 14-3-3γ knockout mice after inoculation with pathological prion protein. Mol Cell Biol 2005;25:1339–46

ELSEVIER

Journal of Neuroscience Methods xxx (2005) xxx–xxx

JOURNAL OF NEUROSCIENCE METHODS

www.elsevier.com/locate/jneumeth

Rapid identification of 14-3-3-binding proteins by protein microarray analysis

Jun-ichi Satoh[a,b,*], Yusuke Nanri[a], Takashi Yamamura[a]

[a] *Department of Immunology, National Institute of Neuroscience, NCNP, 4-1-1 Ogawahigashi, Kodaira, Tokyo 187-8502, Japan*
[b] *Department of Bioinformatics and Neuroinformatics, Meiji Pharmaceutical University, 2-522-1 Noshio, Kiyose, Tokyo 204-8588, Japan*

Received 8 June 2005; received in revised form 19 September 2005; accepted 26 September 2005

Abstract

The 14-3-3 protein family consists of acidic 30-kDa proteins composed of seven isoforms in mammalian cells, expressed abundantly in neurons and glial cells of the central nervous system (CNS). The 14-3-3 isoforms form a dimer that acts as a molecular adaptor interacting with key signaling components involved in cell proliferation, transformation, and apoptosis. Until present, more than 300 proteins have been identified as 14-3-3-binding partners, although most of previous studies focused on a limited range of 14-3-3-interacting proteins. Here, we studied a comprehensive profile of 14-3-3-binding proteins by analyzing a high-density protein microarray using recombinant human 14-3-3 epsilon protein as a probe. Among 1752 proteins immobilized on the microarray, 20 were identified as 14-3-3 interactors, most of which were previously unreported 14-3-3-binding partners. However, 11 known 14-3-3-binding proteins, including keratin 18 (KRT18) and mitogen-activated protein kinase-activated protein kinase 2 (MAPKAPK2), were not identified as a 14-3-3-binding protein. The specific binding to 14-3-3 of EAP30 subunit of ELL complex (EAP30), dead box polypeptide 54 (DDX54), and src homology three (SH3) and cysteine rich domain (STAC) was verified by immunoprecipitation analysis of the recombinant proteins expressed in HEK293 cells. These results suggest that protein microarray is a powerful tool for rapid and comprehensive profiling of 14-3-3-binding proteins.

Keywords: 14-3-3-Binding protein; Immunoprecipitation; Protein microarray; Protein–protein interaction; STAC

1. Introduction

The 14-3-3 protein family consists of evolutionarily conserved, acidic 30-kDa proteins composed of seven isoforms named β, γ, ε, ζ, η, θ, and σ in mammalian cells. A homodimeric or heterodimeric complex composed of the same or distinct isoforms constitutes a large cup-like structure possessing an amphipathic groove with two ligand-binding capacity (Fu et al., 2000; van Hemert et al., 2001). The dimeric complex acts as a molecular adaptor that interacts with key signaling molecules involved in cell differentiation, proliferation, transformation, and apoptosis. It regulates the function of target proteins by restricting their subcellular location, bridging them to modulate catalytic activity, and protecting them from dephosphorylation or proteolysis (Dougherty and Morrison, 2004; MacKintosh, 2004). Although 14-3-3 is widely distributed in neural and non-neural tissues, it is expressed most abundantly in neurons in the central nervous system (CNS), where it represents 1% of total cytosolic proteins (Berg et al., 2002). Aberrant expression and impaired function of 14-3-3 in the CNS are associated with pathogenetic mechanisms of Creutzfeldt–Jacob disease, Alzheimer disease, Parkinson disease, spinocerebellar ataxia, amyotrophic lateral sclerosis, and multiple sclerosis (Chen et al., 2003; Kawamoto et al., 2002; Layfield et al., 1996; Malaspina et al., 2000; Satoh et al., 2004; Zerr et al., 1998).

In general, the 14-3-3 protein interacts with phosphoserine-containing motifs of the ligands such as RSXpSXP (mode I) and RXXXpSXP (mode II) in a sequence-specific manner (Dougherty and Morrison, 2004; MacKintosh, 2004). Previously, more than 300 proteins have been identified as being 14-3-3-binding partners. They include key signaling components, such as Raf-1 kinase, Bcl-2 antagonist of cell death (BAD), protein kinase C (PKC), phophatidylinositol 3-kinase (PI3K), and cdc25 phosphatase (Fu et al., 2000; van Hemert et al., 2001). Binding of 14-3-3 to Raf-1 is indispensable for its kinase activity in the Ras-MAPK signaling pathway, and the interaction of 14-3-3 with BAD, when phosphorylated by

* Corresponding author. Tel.: +81 42 341 2711; fax: +81 42 346 1753.
E-mail address: satoj@ncnp.go.jp (J.-i. Satoh).

0165-0270/$ – see front matter © 2005 Published by Elsevier B.V.
doi:10.1016/j.jneumeth.2005.09.015

a serine/threonine kinase Akt, inhibits apoptosis. Recent studies indicate that the 14-3-3 protein could interact with a set of target proteins in a phosphorylation-independent manner (Dai and Murakami, 2003; Henriksson et al., 2002; Zhai et al., 2001). Increasing knowledge of interactions between 14-3-3 and interacting molecules would help us to understand the biological function and pathological implication of the 14-3-3 protein networks.

The yeast two-hybrid (Y2H) system is a powerful approach to identify novel protein–protein interactions. However, Y2H screening requires a lot of time and effort, and is often criticized for detecting the interactions unrelated to the physiological setting and obtaining high rates of false positive interactors caused by spontaneous activation of reporter genes and self-activating bait proteins (Vidalain et al., 2004; Zhang et al., 2004). Affinity purification coupled with mass spectrometry (APMS) is an alternative approach to identify the components of protein complexes on a large scale. This approach has been taken to identify a wide variety of 14-3-3-interacting proteins involved in cell proliferation, metabolism, and survival (Benzinger et al., 2005; Jin et al., 2004; Meek et al., 2004; Pozuelo Rubio et al., 2004). Although the APMS procedure detects binding partners of physiological significance, it is laborious and has a difficulty in detecting transmembrane proteins and loosely associated components that might be lost during purification (von Mering et al., 2002). Recently, protein microarray technology has been established for rapid, systematic, and less expensive screening of thousands of protein–protein, protein–lipid, and protein–nucleic acid interactions in a high-throughput fashion. This approach has important applications in the areas not only of basic biological research but also of drug discovery research, including identification of the substrates of protein kinases and the protein targets of small molecules (Chan et al., 2004; MacBeath and Schreiber, 2000; Michaud et al., 2003; Zhu et al., 2001).

The present study was designed for the first time to identify a comprehensive profile of human 14-3-3-binding proteins by analyzing a high-density protein microarray.

2. Materials and methods

2.1. Preparation of a probe for microarray analysis

Human embryonic kidney cells HEK293 whose genome was modified for the Flp-In system (Flp-In 293) were obtained from Invitrogen, Carlsbad, CA. Flp-In 293 cells contain a single Flp recombination target (FRT) site targeted for the site-specific recombination, integrated in a transcriptionally active locus of the genome, where it stably expresses the *lacZ*-Zeocin fusion gene driven from the pFRT/*lac*Zeo plasmid under the control of SV40 early promoter. Flp-In 293 cells were maintained in Dulbecco's modified Eagle's medium (DMEM) supplemented with 10% fetal bovine serum (FBS), 100 U/ml of penicillin, and 100 μg/ml of streptomycin (feeding medium) with inclusion of 100 μg/ml of Zeocin (Invitrogen) as described previously (Satoh and Yamamura, 2004).

To prepare the probe for protein microarray analysis, the open reading frame (ORF) of the human 14-3-3ε gene (YWHAE) was amplified from cDNA of NTera2-N cells (Satoh and Kuroda, 2000) by PCR using PfuTurbo DNA polymerase (Stratagene, La Jolla, CA, USA) and the primer sets listed in Table 1. The PCR product was then cloned into a mammalian expression vector pSecTag/FRT/V5-His TOPO (Invitrogen) to produce a fusion protein with a C-terminal V5 (GKPIPNPLLGLDST) tag, a C-terminal polyhistidine (6 × His) tag, and an N-terminal Ig κ-chain secretion signal. This vector, together with the Flp recombinase expression vector pOG44 (Invitrogen), was transfected in Flp-In 293 cells by Lipofectamine 2000 reagent (Invitrogen). A stable cell line was established after incubating the transfected cells for approximately 1 month in the feeding medium with inclusion of 100 μg/ml of Hygromycin B (Invitrogen). It was named 293 eV5. The recombinant protein was secreted into the culture medium of 293 eV5 cells after the Ig κ-chain secretion signal sequence was processed by an endogenous signal peptidase-mediated cleavage.

To purify the recombinant 14-3-3ε protein, the culture supernatant of 293 eV5 cells incubated for 48 h in the serum-free DMEM/F-12 medium was harvested and concentrated at an 1/40 volume by centrifugation on an Amicon Ultra-15 filter (Millipore, Bedford, MA). It was then purified by the HIS-select spin column (Sigma, St. Louis, MO) and concentrated at an 1/10 volume by centrifugation on a Centricon-10 filter (Millipore). The protein concentration was determined by a Bradford assay kit (BioRad, Hercules, CA). The purity and specificity of the probe were verified by Western blot analysis using mouse monoclonal anti-V5 antibody (Invitrogen) and rabbit polyclonal antibody specific for the 14-3-3ε isoform (IBL, Gumma, Japan).

2.2. Protein microarray analysis

ProtoArray human protein microarray (v1.0) commercially available from Invitrogen was utilized in the present study. It contains 1752 human proteins of various functional classes spotted in duplicate on a nitrocellulose-coated glass slide. To prepare target proteins immobilized on the microarray, an N-terminal glutathione-*S* transferase (GST)-6× His fusion protein derived from the genes selected from the human ultimate ORF clone collection (Invitrogen) was expressed in Sf9 insect cells by using the baculovirus expression system (Invitrogen). Either the full-length or the partial fragment of recombinant proteins, was purified under native conditions by glutathione affinity chromatography in the presence of protease inhibitors, then processed for spotting on the slides. The proteins were printed in an arrangement composed of 4 × 12 subarrays equally spaced in vertical and horizontal directions (Fig. 1a). Each subarray included 16 × 16 spots, composed of 48 control spots (C), 80 human proteins (H), and 128 blanks (B) (Fig. 1c). The control proteins (C) were composed of 14 positive control spots and 34 negative control spots. The former includes four spots of an Alexa Fluor 647-labeled antibody (rows 1, 8; columns 1, 2), six spots of a concentration gradient of a biotinlyated anti-mouse antibody with a capacity to bind to mouse monoclonal anti-V5 antibody conjugated with Alexa Fluor 647 (row 8; columns 3–8), and four spots of a concentration gradient of V5 protein (row 8; columns 13–16). The latter includes six spots of a concentra-